Aggregation and Control of Flexible Thermal Demand for Wind Power Based Power System Analysis

Master Thesis
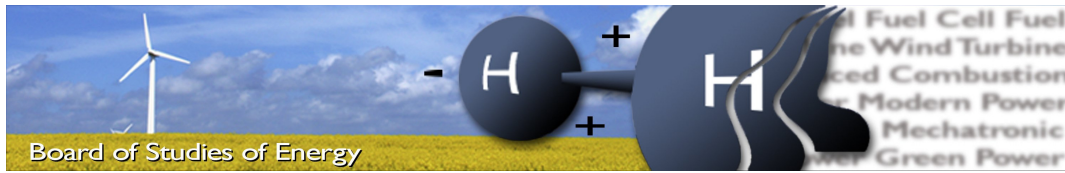Helma Maria Tróndheim

Board of Studies of Energy

Title:	Aggregation and Control of Flexible Thermal Demand for Wind Power Based Power System Analysis
Semester:	10th Semester
Semester theme:	Master Thesis
Project period:	01.02.18 to 01.06.18
ECTS:	30
Supervisors:	Jayakrishnan Radhakrishna Pillai and Sanjay Chaudhary
Project group:	EPSH4-1037

Helma Maria Tróndheim

SYNOPSIS:

The Faroese government is aiming for a 100 % renewable onshore energy sector by 2030. To reach this goal, the amount of installed wind power will increase significantly. This results in some challenges regarding the stability of the power system. Additionally, transport and heating will be electrified. The electrification of heating, will increase the number of heat pumps in the grid. These heat pumps can possibly contribute to the stability issues caused by the large penetration of wind power, due to their inherent hot water storage. This can be done by implementing a load frequency controller which controls the heat pumps in addition to the generating units. This thesis investigates the possibility of using heat pumps to provide secondary frequency regulation in an island power system. Dynamic simulations are conducted in order to obtain the frequency of the power system with different stages of integrated wind power.

Pages:	71
Appendix:	A, B & C

Preface

This thesis has been written by Helma Maria Tróndheim (EPSH4-1037) on the 10th semester at the Department of Energy Technology at Aalborg University, from the 1st of February 2018 to the 1st of June 2018. The thesis investigates the potential contribution from flexible thermal demand to supplementary frequency control in a wind power based power system.

I would like to gratefully acknowledge the patient guidance and support from my supervisors Jayakrishnan Radhakrishna Pillai and Sanjay Chaudhary. Furthermore, Kári Mortensen (The Faroese Environment Agency) and Terji Nielsen (The Power Company SEV) are thanked for provision of data.

The software DIgSILENT PowerFactory has been used to model and simulate a transmission grid with its elements. Additionally, Matlab has been used to analyse data. The project is written in LaTeX.

Reader's Guide The project is based on information from literature, web pages and reports. The sources are cited in the report using the IEEE citation style, and can be found in References. Tables, figures and equations are labeled with the number of the chapter.

Abstract

Introducing more renewable power into power system creates challenges regarding the stability of the grid. As conventional units are removed, new methods for e.g. frequency regulation will have to be employed This investigation focuses on using heat pumps in a wind dominated power system for load frequency control. The maximum wind share achieved was a daily share of 50 %.

A grid with conventional and renewable units has been modelled, and dynamic simulations have been conducted with load frequency control. The load frequency controller was proven to be efficient, since it is capable of restoring the frequency back to 50 Hz after a power deficit has occurred. The frequency was kept within 49.87 Hz and 50.07 Hz, when the grid frequency was tested wth a hourly based load profile, and with load frequency control from a diesel and hydro generator. The addition of wind power increased the frequency deviations from the nominal value to be between 49.5 Hz and 50.3 Hz. The introduced wind power can therefore be said to affected the frequency balance negatively.

A heat pump model has been developed and the behavior was validated through tests. Even though the behavior of the controllers and heat pump model was validated, the usage of heat pumps in the load frequency control has not been proven very efficient in this study case. There are some improvements on the frequency, but these are however very small, and can be considered negligible. The minimum and maximum frequencies reached were in general not improved. The limitations of the controller and the relatively stable frequency are considered to be part of the reason why the improvements are so small. All simulations were conducted based a winter and a summer day, with different levels of wind power integration. The simulations are based on measured load, weather data and heat demand of a heat pump.

List of Figures

List of Tables

Nomenclature

Symbol	Unit	Description
A_R	m^2	Rotor's swept area
B	MW/Hz	Frequency Bias Factor
C_P	-	Power coefficient
COP	-	Coefficient of Performance
f	Hz	Frequency
f_n	Hz	Nominal frequency
f_ss	Hz	Steady state freqeuncy
k_pf	-	Frequency dependency coefficient
k_put	-	Voltage dependency coefficient
N	-	Number of heat pumps
P_CPP	MW	Conventional power plant power
P_HPP	MW	Hydro power plant power
P_HP	MW	Heat pump power
P_L	MW	Load
P_L0	MW	Initial load
P_n	MW	Nominal Power
P_WT	W	Wind turbine power
p_{lfc}	MW	Load frequency control signal
p_{gov}	p.u.	Governor signal
R	p.u.	Droop
U	V	Voltage
v	m/s	Wind speed
β	MW/Hz	Frequency Characteristics
ΔP	-	Power Deficit
ρ	kg/m^3	Air density
τ_r	s	Rate limiter time constant

Abbreviation	Description
AVR	Automatic Voltage Regulator
COP	Coefficent of Performance
CPP	Conventional Power Plant
DSM	Demand Side Management
HPP	Hydro Power Plant
HP	Heat Pump
HPS	Heat Pump System
LFC	Load Frequency Control
RES	Renewable Energy Sources
TSO	Transmission System Operator
WF	Wind Farm
WT	Wind Turbine

Contents

Chapter 1

Introduction

This chapter introduces the topic at hand. First the background to the project is described with a short introduction to renewable energy and demand side management. The problem formulation of the project with the main objectives, applied methodology and limitations of the project are stated. Finally, the outline of the thesis is represented.

1.1   Background

The awareness of climate changes due to air pollution from e.g. power production, has increased the interest of implementing renewable energy in power systems. According to [1], the installed capacity of wind power is increasing faster than the capacity of other renewable technologies available.

In October 2014 the Faroese power company SEV announced, that it is aiming for an 100 % renewable onshore energy sector by 2030 [2]. A year later this was supported by the government in the coalition agreement [3]. Not only will the electricity production have to be 100 % renewable, but the fossil fueled heating and transport will have to be replaced by renewable solutions. With a 100 % renewable power production, an electrification of these two is one possible renewable solution .

Reference [4] presents a possible 100 % renewable energy mix in the Faroe Islands in 2030. The study suggests that 35 % of the capacity in 2030 should be wind power, 20 % hydro power, 15 % solar power, and 30 % tidal power. A newer study however states, that tidal power will be too expensive compared to other sources in the upcoming years. Therefore it is suggested that solar and wind power should be the dominating energy sources [5].

Figure 1.1 [4] shows simulation results for the production in 2030. The load in 2030 is projected to be 593 GWh. On the figure the production from each source type is shown individually. The total production is 729 GWh, with 137 GWh excess and 93 GWh shortage. The RES share of the production is 84 %, and this is calculated based on how much of the

load is covered by the production.

Data from the production in 2015 show that a total of 314 GWh were produced, of which 60 % were produced by renewable energy sources (RES) [4]. It is estimated that the production could have an excess of 10 GWh, however this was curtailed. Therefore it can be stated that the excess production, is likely to increase significantly, from 10 GWh to 137 GWh.
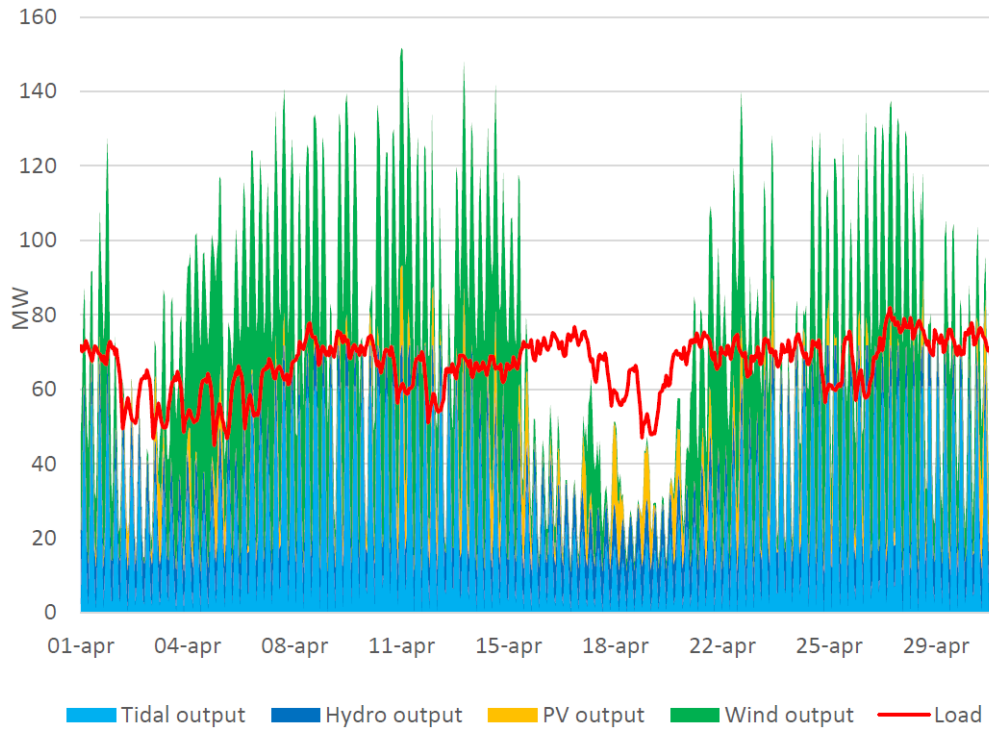
Figure 1.1: Simulation results of production in 2030. The production from each source type is shown individually together with the the total load [4].

Ancillary services, which are services supporting the electric transmission from generation to consumption [6], are traditionally provided by synchronous machines. A high share of inverter based RES, e.g. wind turbines (WT) or photo voltaic (PV) panels, will therefore lead to challenges regarding the power quality, reliability and stability on power systems [7], and new methods to provide these services will have to be implemented.

Distributed generation together with electrification of heating and transport can also have some disadvantages to the grid, especially the distribution grid. Reference [8] states a significant increase of distributed generation, heat pumps (HP) and electric vehicles integrated in power systems will lead to higher power flows at the medium and low voltage, which can cause line congestion and voltage issues.

According to [9] there are four options regarding a high integration of RES. These options are listed in the following bullet points:

- **Grid:** The grid can be reinforced to prevent e.g. line congestion.

- **Supply side management:** Increasing the flexibility of power plants, and gaining a quicker response from them.

- **Storage:** Installing different types of storage can increase the reliability of the grid.

- **Demand side management:** By managing the demand side, it is possible to shift the load, and this can balance the system. Reference [10] even states that it is a necessity that demand is flexible in grid with high integration of RES.

1.1.1 Demand Side Management

Demand side management (DSM) is most commonly used to shift load, and thereby decrease the peak load and increase off peak load. This results in a better balance and higher flexibility of the system [11].

DSM can revolve around different types of loads. Electric vehicles, electric boilers, electrolysers and HP systems all have storage that can enable a high RES integration. Utilizing these large amounts of inherent storages that are currently not utilized, might even be cheaper than installing e.g. large battery systems [12].

As it is expected that the amount of HP, on the grid will increase significantly, it is interesting to investigate what they can contribute with on transmission level. Studies show that heat pumps can contribute to frequency stability in power systems [11, 12].

Reference [13] states that if the transmission system operator (TSO) can control the heat pump, a few hours can pass without the customer's comfort being decreased, depending on the size of the thermal storage of the heat pump system and the customer's comfort requirements. However, there are some technical issues for enabling this. The HP sytems are distributed and have to be aggregated. They have to be controlled and coordinated in a smart way, and at the same time be economically feasible. This thesis aims to investigate how an aggregated HP system can contribute with frequency regulation in a power system with a high integration of wind power.

1.2 Problem Formulation

The amount of heat pumps where district heating is not a possibility is expected to increase. Large heat pump units can also replace the production from units at district heating power plants, during periods when e.g. there is excess wind power. These units have thermal storage that can be used for active power regulation of the demand side, and facilitating system balancing on the supply side. Heat pumps are being considered for future grid support and ancillary services, due to their flexible operation. The project will focus on the behaviour of heat pumps, and their possible impact on power system operation. An appropriate heat pump model will be developed for the study considered. Additionally,

aggregation and control techniques will be developed for ensuring the flexible participation of heat pumps for power system balancing in a grid with large amounts of renewable power generation like wind turbines.

1.3   Objectives

The main aim of this thesis is to investigate how the thermal storage of an aggregated heat pump system, can contribute with frequency regulation to the grid. The objective will be fulfilled through the following tasks:

- Investigate and understand the electrical and basic thermal behaviour of heat pumps.
- Create simplified heat pump model whose consumption pattern can easily and realistically be aggregated at the system level.
- Implement a methodology for aggregating and controlling large amount of thermal load characteristics and elaborate their unified load profile.
- Model suitable test grid and its assets, use and apply control schemes in regulation units for frequency stability studies.
- Dynamic studies: Grid support study, primarily focusing on system frequency response, apply different operational scenarios – excess wind power production and penetration, and seasonal load characteristics.

1.4   Methodology

This project has been conducted using DIgSILENT PowerFactory in an extensive degree. A grid model of the Faroese Power System was provided by DanskEnergi, and has been modified for the purpose of this study. The grid involves three types of generation units, and two types of loads. Dynamic models have been made with the purpose to control the grid elements. A load frequency controller has been employed. RMS simulations have been conducted to investigate the behavior of the modelled grid.

In addition to using PowerFactory, MATLAB has been used to prepare and analyze data for and from PowerFactory, respectively.

The applied methodology is the following:

- Suitable dynamic models of different elements have been applied.
- Each model has been tested separately.
- The different elements have been implemented into the grid.
- A load frequency controller has been designed.
- RMS simulations have been conducted for different scenarios.

1.5 Limitations

The project is limited according to the following list:

- The following generating units have been aggregated to one of each type:
  - Two hydro generators.
  - Four diesel generators.
  - Six/twelve wind turbines (depending on the test scenario).
- The base loads are aggregated to some degree.
- The heat pump model is an aggregated model representing all the heat pumps.
- The total load profile of all the heat pumps is based on actual data from only one house.
- The simulations are conducted for:
  - A winter day.
  - A summer day.
- The investigation is limited to one of 18 islands on the Faroe Islands.

1.6 Outline of the Thesis

The thesis contains the six chapters listed below, and the outline is as follows:

Chapter 1 - Introduction: The topic at hand is introduced. First the background to the project is described, and then problem formulation, objectives, methodology and limitations are stated. Finally the outline of the thesis is represented.

Chapter 2 - State of the Art: A state of the art review of using heat pumps as flexible loads. The basics of frequency regulation theory is explained. Additionally, the Faroese power system and heating sector are introduced.

Chapter 3 - Study Case: Description and Modelling: This chapter describes the study case and the DIgSILENT modelling of it. The modelling consists of a grid, a hydro generator, a diesel generator, a wind turbine and the base loads of the system. The models are described and tested.

Chapter 4 - Load Frequency Controller: In this chapter the applied load frequency controller is explained and tested. The chapter also contains information about load assumptions and adjustment of wind power. Finally simulations results with load frequency control of present generating units with different scenarios are represented.

Chapter 5 - Frequency Regulation with Heat Pumps: This chapter focuses on the design of a aggregated heat pump model and the control of it. The simulation results with the heat pump contributing to frequency regulation for different scenarios are represented.

Chapter 6 - Conclusions and Future Works: The final chapter contains the conclusions of the project, and possible future work based on this thesis..

Chapter 2

State of the Art

This chapter introduces the present electrical power system and the heating sector on the Faroe Islands. Then the basic working principles of a heat pump are explained, followed by frequency regulation theory. Studies of using heat pumps as flexible loads are then discussed. Finally, the chapter is summarized.

2.1 Electrical Power Grid

The archipelago consists of 18 islands with seven isolated electrical power grids. 11 islands are connected to the main grid, six islands have individual grids, while the final island is uninhabited; therefore, it does not have a power supply. Figure 2.1 shows a map of the Faroe Islands, where the islands that are connected to the main grid, and the ones which are isolated electrically are marked. The installed capacity separated into conventional power plants (CPP), hydro power plants (HPP), and wind power plants (WPP) is also shown on the figure, together with the size of the battery energy storage system (BESS) on the islands.

The total installed capacity on the grid is 124.6 MW. The shares between the different types of sources are the following: 52.6 % CPPs, 32.6 % HPPs, and 14.8 % WPPs. The production shares differ from the capacity shares. In 2015 a total of 314 GWh were produced. CPPs provided 39.9 %, HPPs 42.3 %, and WPPs 17.8 % [4].

The voltage levels in the Faroe Islands are 60 kV, 20 kV, 10 kV, 6 kV and 0.4 kV. The location and amount of the first four voltage levels are shown on Figure 2.2 [14]. 60 kV is used for transmission between the power plants on the main grid and substations. 20 kV, 10 kV and 6 kV are used for distribution at differnet locations.

Figure 2.1: A map of the Faroe Islands, that shows the seven electrical power grids together with installed capacities of conventional power plants, hydro power plants, wind power plants, and battery energy storage systems.

(a) 60 kV   **(b)** 20 kV   **(c)** 10 kV   **(d)** 6 kV

Figure 2.2: The voltage levels in the Faroe Islands [15].

2.1.1 The Electrical Power Company SEV

The Electrical Power Company SEV is owned by all the municipalities in the Faroe Islands, and is obliged to provide reliable electricity to the whole country. It has monopoly on both transmission and distribution, and the company also produces most of the power, as 98 % of the installed capacity is installed and run by SEV.

SEV is aiming for a 100 % renewable onshore energy sector by 2030. However, SEV does not have the authority to demand customers to switch to e.g. heat pumps and electric vehicles. Hence, the only thing the company can do regarding the electrification is to be prepared to provide the necessary services, and to encourage the customers to choose renewable solutions. This being said; the government, which is the superior authority, has supported SEV's goal in the Coalition Agreement from 2015 [3], as mentioned previously. The first initiative from the government regarding this subject, has however not been taken until recently, when a proposal that will give SEV the authorization to charge customers with HPs and electric vehicles with lower electricity prices was submitted to the parliament by the Minister of Energy [16]. If passed, it will be possible for consumers to charge their electric vehicles at night for a lower price, while the power consumed by the heat pump will charged at lower price at all times. The bill suggests a price reduction of 0.5 DKK/kWh. The strategy is to encourage customers to switch to HPs and electric vehicles, in addition to even the load by charging at night.

The current electricity price in the Faroe Islands is generally fixed at 1.76 DKK/kWh. There are however some variations of the price for larger consumers, and these variations also depend on the customer type, see Table 2.1 [15].

Table 2.1: Electricity prices 2018 including value added taxes (VAT) categorized by customer type and annual consumption [15].

Customer type	Annual consumption [kWh]	Price incl. VAT [DKK/kWh]
Nonindustry	0 to 10 000	1.76
	10 000 to 100 000	1.66
	over 100 000	1.61
Industry	0 to 10 000	1.76
	10 000 to 30 000	1.66
	over 30 000	1.38

2.2 Heating Sector

Figure 2.3 shows the distribution of the different types of heat sources in households in the Faroe Islands. The figure is based on statistics from a 2011 census [17]. A total of 17441 households participated in the census, of which 6 % did not state their type of heating

source. From the figure it is obvious that most households (85 %) in the Faroe Islands are heated by oil or gas burners, while only 4 % have HPs or electric boilers. The amount of households with oil burners is significantly higher than in e.g. Denmark were this technology will be phased out in a few years time. The district heating grid in the Faroe Islands, which is explained further in subsection 2.2.2, covers 5 % of the households. A negligible number of houses use wind power, solar power, or wood for heating.
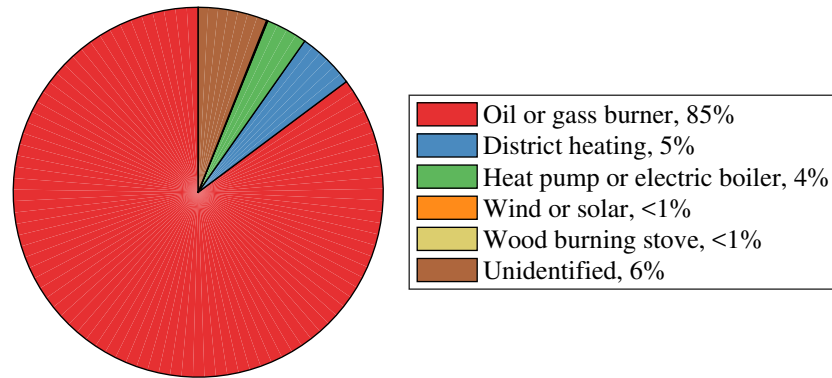
Figure 2.3: Distribution of the different types of heat sources in Faroese households in 2011, based on [17].

Considering that the data Figure 2.3 are based on are from 2011, it is likely that the distribution has changed. It is estimated that there today are 18000 households, 89 % with oil burners, 5.5 % on the district heating grid and 5.5 % with HPs. All other sources are assumed to be negligible [18]. The oil burners burn 36000 tons of oil annually, which is 360 GWh [17]. In the 2011 data 6 % were unidentified; hence, it is not possible to compare the numbers directly. If these households and the ones with solar/wind/wood are ignored, and the shares are recalculated it is possible to compare. In other words; 16372 households from the 2011 census are considered for comparison. 91 % of which have oil burners, 5 % are on the district heating grid and 4 % have HPs. From these numbers it is clear that amount of heat pumps with respect to the total number of households has increased slightly. This increase is expected to continue, as people are becoming more aware of the advantages of installing a heat pump instead of an oil burner, see subsection 2.2.1.

2.2.1 Heat Pumps

There are several types of HPs available. The cheapest solution is a air-to-air HP. These utilize the outdoor temperature and blow warm air inside. These are however not considered as a solution that provides comfort by many, due to the blowing air. This type is not relevant for the study either, due to the lack of thermal storage. Other types instead heat water, which is then used to heat the building. Three sources are used in the Faroe Islands, air, ground and seawater. Air source HPs are according to [19] the best fitted for households. They are not as expensive as ground source HPs, but not as efficient either. There are approximately 230 ground source HP systems in the Faroe Islands, while the

rest is mainly air source. There are a few seawater based systems, but these are in larger buildings.

Figure 2.4 [20] shows a diagram with the working principle of an air-to-water HP system overview. The HP utilizes the temperature of the source, in this case air. These types of HPs have an outdoor unit and an indoor unit. Refrigerant runs through a pipe in the outdoor unit, and takes heat from the air, which is then compressed to a higher temperature. The now gaseous refrigerant goes through the indoor unit, where it heats the water in the hot water storage tank. The heat condensates releasing the latent heat and runs back to the outdoor unit.
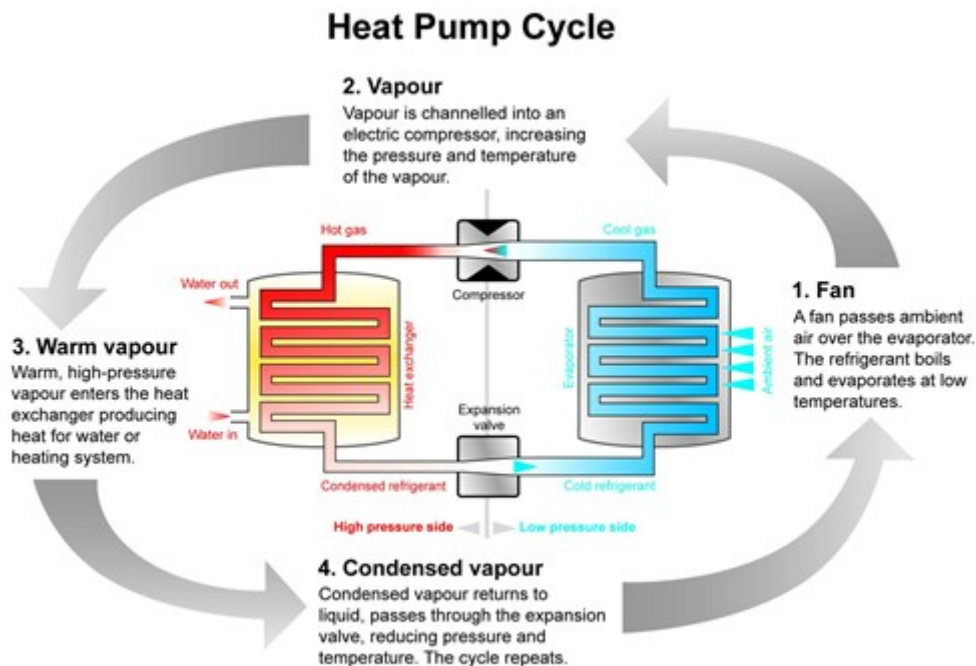
Figure 2.4: A diagram of a heat pump with the basic working principle [20].

There are technical and environmental advantages with HP compared to e.g. oil burners. The most significant technical advantage is the high coefficient of performance (COP), i.e. the HPs are more efficient than oil burners. A HP typically has a COP of 3 to 5, while the efficiency of a efficient oil burner is 95 % to 98 % [21]. As for the environmental advantages, a HP can be considered renewable when the power production is renewable.

2.2.2 District Heating

In 2011 5 % of the households in the Faroe Islands were connected to a district heating grid, which is located in the capital area. The grid is shown on Figure 2.5 (2013) [22]. Every new house built in the area, where the district heating grid is, is required to connect to it.

The district heating heat is partly received from a incineration station. Waste is burned at a temperature, that has to be lowered before the smoke can go through the chimney. Instead of cooling the temperature, it used for district heating. SEV's largest CPP is also connected to the district heating grid. The warm cooling water of the engines is delivered to the district heating grid. In addition to the incineration station and the CPP, there is a backup system when e.g. no waste is being burned, or when the CPP is out of service [22].
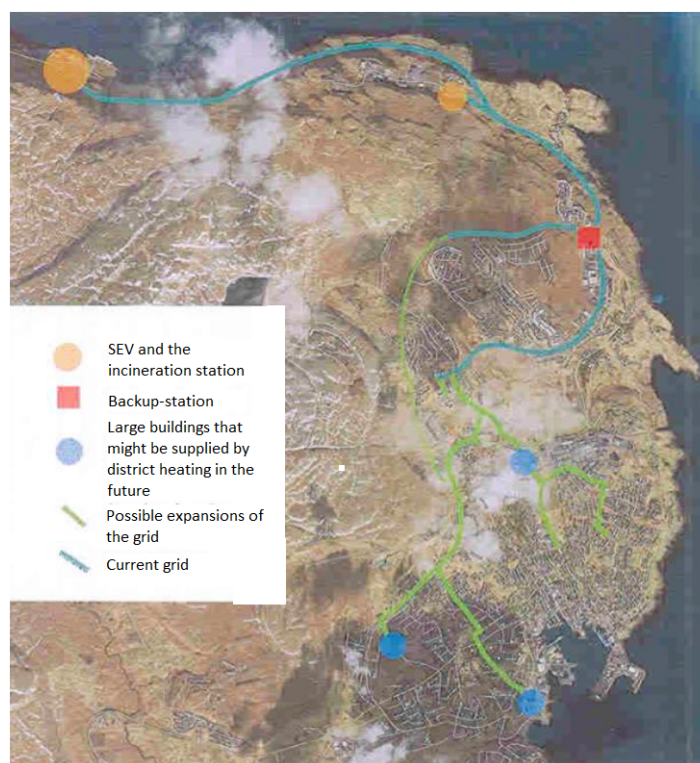
Figure 2.5: The district heating grid in 2013 [22].

2.2.3 A Typical Household

In this section heating data from a typical household will be represented. The household's heating source is a 6 kW HP [18].

Figure 2.6 shows how the average daily electricity consumption by the HP throughout a year together with the outside temperature. It can be seen that it is required to heat the

house all year around, and this is due to the relatively low temperatures in the summer.
50 % of the data is between 15 kWh and 24 kWh.
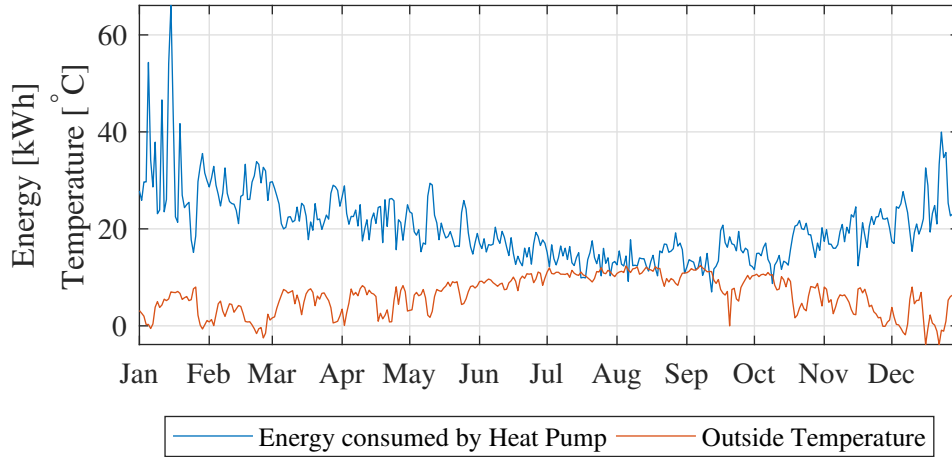
Figure 2.6: Average daily outside temperature and daily electricity consumed by heat pump in a typical household over a year [18].

On Figure 2.7 the hourly electricity consumption by the heat pump is shown. It is the average profile over a year.
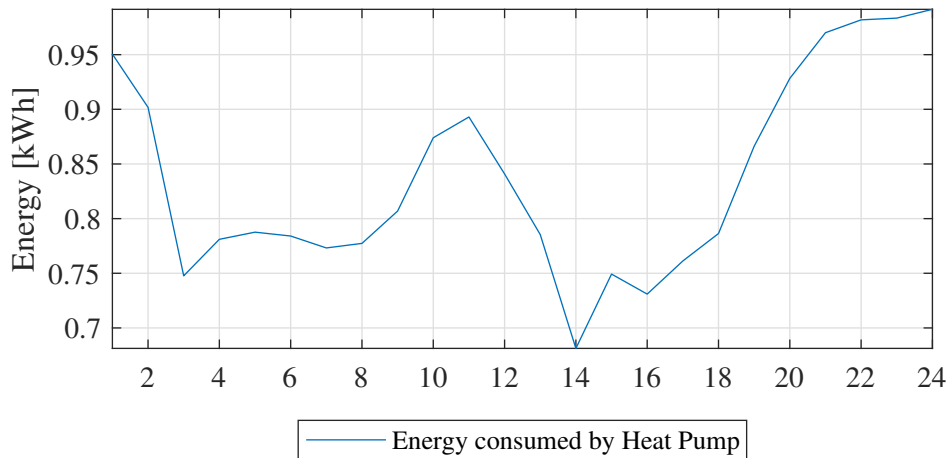
Figure 2.7: Average hourly electricity consumed by heat pump [18].

In addition to the two profiles presented, the data also showed that 84 % of the energy was used for central heating while 16 % was used for hot water. This data is only available as an average daily value, and it was seen that it remained constant throughout the year.

2.2.4 Future Heating Sector

A 100 % renewable energy sector requires the 16000 oil burners to be replaced by e.g.
HP. In 2016 the possibilities to convert the heating in a whole village, Leirvík, from fossil
fuels to a renewable solution were investigated by the consulting engineers COWI A/S.
The investigation was a part of Nordic Energy Sources' project called "Sustainable energy
and energy storage in sparsely populated areas". Different scenarios were investigated
and compared to the current most common source; Oil burners. The scenarios were the
following:

- **Scenario 1:** Individual heat pumps, individual brine.
- **Scenario 2:** Individual heat pumps, shared brine.
- **Scenario 3:** Seawater heat pump, district heating.

Figure 2.8 [23] shows the results from the investigation. Scenario 3 is the most profitable
solution, while the most common solution today is the most expensive. The difference
between the traditional method, and all three heat pump solutions is the initial investment
price and the price for the actual heating (oil/electricity). These results show that even
though electrification initially is expensive, it is the most feasible solution over time, so
not only is it renewable, considering the power production is renewable, but it is also
profitable. This should encourage people to electrify their heating system.
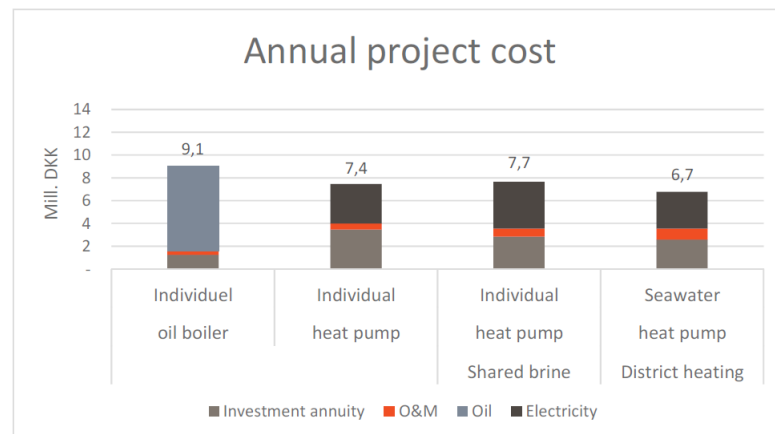
Figure 2.8: The annual project costs in the three scenarios compared to oil burners. O&M is short for
operation and maintenance. The electricity prices were assumed to be lower in the night than during
the day [23].

2.3 Frequency Regulation

Frequency regulation is an important part of power system operation, as it aims to main-
tain a close-to-constant frequency. With the increase of renewable sources it becomes even

more important, as these sources result in a less stable grid. This is due to their fluctuating production and lack of capability to provide frequency regulation automatically.

Frequency regulation is divided into three stages; primary, secondary and tertiary, and is overall often refereed to as load frequency control (LFC). The primary frequency control stabilizes the frequency after a contingency. This is an automatic control, that has to be conducted within 30 seconds after a contingency. After the frequency has been stabilized it has to be restored to its nominal value, this is the secondary frequency control. Secondary control can be automatic or manual, and has to be deployed within 15 minutes of the contingency. Finally the frequency is supported by the tertiary frequency reserve, which is a manual control. The mentioned limits are valid for grids on the European Network of Transmission System Operators for Electricity (ENTSO-e). There are no official time limits of frequency regulation deployment for the Faroese power system. Figure 2.9 illustrates the three regulation stages, together with the standards for ENTSO-e networks. The automatic primary and secondary controls are described in details in the following sections [24].
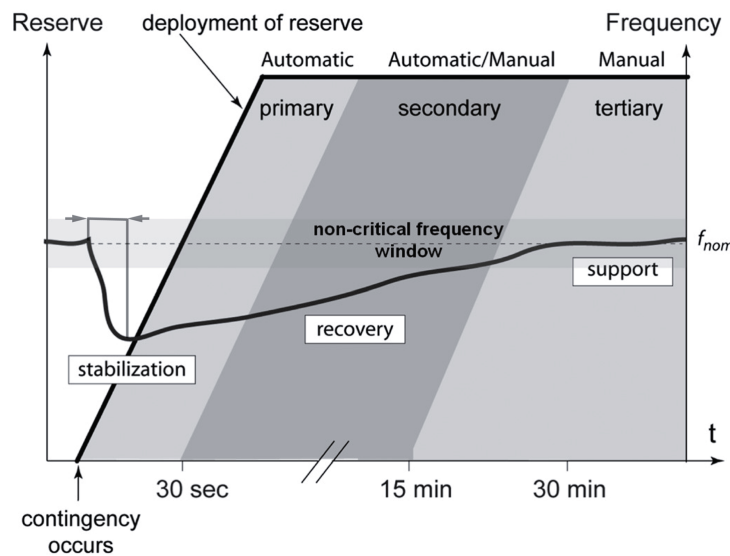
Figure 2.9: Frequency regulation standards for ENTSO-e networks [24].

2.3.1 Primary Frequency Control

In typical power system operation the primary frequency control is done by governors of the conventional power plants. A governor detects a frequency deviation and regulates the input to the turbine, ΔP_V, accordingly. Figure 2.10 [25] shows a block diagram of a simple system with a primary control. It consists of a generator, the load, a prime mover and a governor.

The governor is represented by a time constant, τ_g, and a droop constant, R. The droop constant is the change in speed divided by the change in power $R = \Delta\omega/\Delta P$. The input to the governor, ΔP_g, is change in power reference set point minus the feedback signal of the

system, $\Delta P_g = \Delta P_{ref}(s) - \frac{\Delta\Omega(s)}{R}$, and the output is the change in valve position ΔP_V. The turbine in the block diagram is a nonreheat steam turbine, which is the simplest model, as it can be modelled by a single time constant, τ_T. The output of the turbine is the change in mechanical power, ΔP_m. The load of a system can be modelled by $\Delta P_e = \Delta P_L + D\Delta\omega$. ΔP_L is the nonfrequency-sensitive loads e.g. lighting, while $D\Delta\omega$ are the frequency-sensetive loads e.g. motors. If the load change 0.6 % due to a 1 % change in frequency, the damping factor, D, is 0.6. The generator itself is represented simply by $1/(2Hs)$, with $\Delta P_m - \Delta P_e$ as the input and $\Delta\Omega(s)$ as the output. H represents the inertia constant of machine [26].
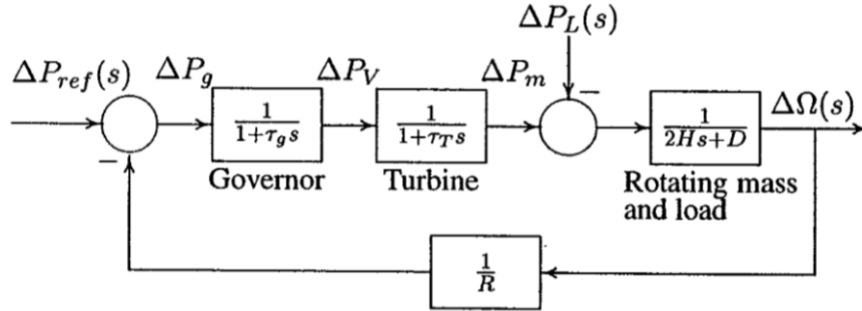
Figure 2.10: Primary control block diagram of an isolated power system [25].

The closed loop transfer function of the system relating $\Delta\Omega(s)$ and $\Delta P_L(s)$ is shown in Equation 2.1 [25].

$$\frac{\Delta\Omega(s)}{-\Delta P_L(s)} = \frac{(1+\tau_g s)(1+\tau_T s)}{(2Hs + D)(1+\tau_g s)(1+\tau_T s) + 1/R} \tag{2.1}$$

As the droop control is a proportional controller, it results in a steady state error, this error is defined by Equation 2.2 known as the final value theorem [25].

$$\Delta\omega_{ss} = \lim_{s\to 0} s\Delta\Omega(s) = (-\Delta P_L)\frac{1}{D + 1/R} \tag{2.2}$$

All units on the Faroese grid are droop controlled.

2.3.2   Secondary Frequency Control

The purpose of secondary frequency control is, as previously mentioned, to restore the frequency to its nominal value. On the Faroese grid secondary control is deployed manually, but with a high integration of RES and DG, the need for an automatic control will increase [25].

In order to control generating units to automatically provide secondary control an integrator is added to the control, as seen on Figure 2.11. The controller gain, K_I, can be adjusted

according to satisfactory transient response [25].
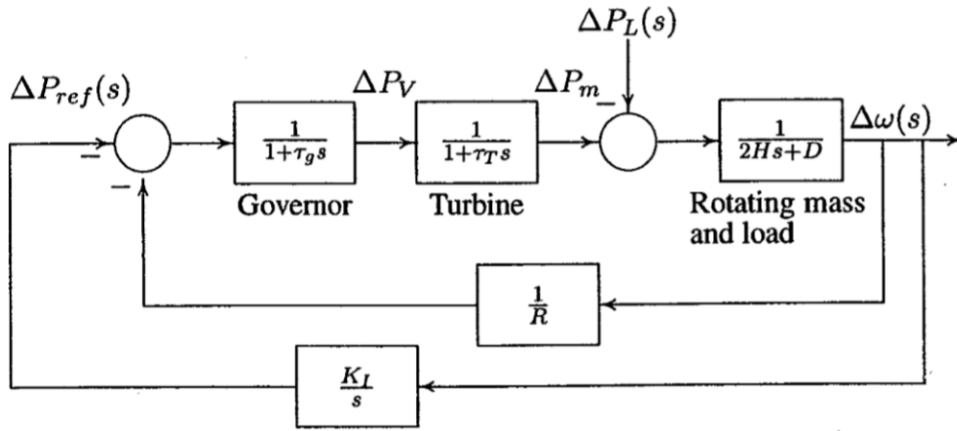
Figure 2.11: LFC block diagram of an isolated power system [25].

The closed loop transfer function of the new system relating $\Delta\Omega(s)$ and $\Delta P_L(s)$ is shown in Equation 2.3 [25].

$$\frac{\Delta\Omega(s)}{-\Delta P_L(s)} = \frac{s(1+\tau_g s)(1+\tau_T s)}{s(2Hs+D)(1+\tau_g s)(1+\tau_T s) + K_I + s/R} \tag{2.3}$$

Figure 2.12 illustrates the difference a LFC makes regarding the frequency response of a system after a contingency. It is clear that the steady state error is zero.
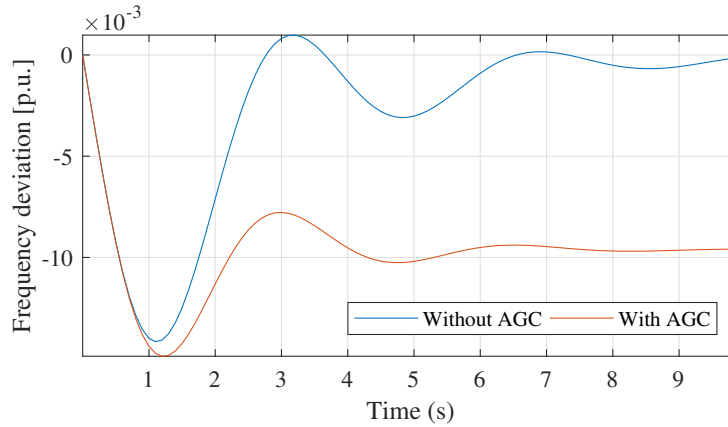
Figure 2.12: Frequency response with secondary control (blue) and without secondary control (red).

Demand side management (DSM) can contribute to secondary control and as an alternative to the replaced conventional generation frequency reserves that will be phased out due to

increased share of renewables. DSM can consist of several demand types as mentioned in subsection 1.1.1, whereof HPs are one option. Implementation of DSM on ENTSO-e networks requires that the DSM ignores small frequency deviations within the deadband specified the respective TSO, and that the DSM unit should react rapidly [27].

2.3.3 Frequency Requirement for Faroese Power Plants

It is desired to keep the frequency on the Faroese grid between 49.5 Hz and 50.5. In addition to this, the power plants should be capable of operating for a certain duration at higher and lower frequencies. These are tabulated in Table 2.2 [28]. This shows that stations should be able to operate between a frequency range of 47 Hz and 52 Hz.

Frequency	47.0-47.5	47.5-49.0	49.0-51.0	51.0-51.5	51.5-52.0
Minimum time	0-20 seconds	30-90 minutes	Continuous	30-90 minutes	0-15 minutes

Table 2.2: The duration power stations above 11 kW should be capable of operating at different frequencies [28].

2.3.4 Heat Pumps and Frequency Regulations

Several studies have investigated the ability for HPs to provide frequency regulations [12, 19, 29–33]. Some of the studies investigate variable speed HPs, which can provide a variable frequency response, while others consider a ON/OFF control for a simplification.

An investigation of the Japanese grid, showed that HPs can contribute to frequency regulation. This investigation used synchronous machines, EVs, BESS and HPs for regulation. Eventhough the HPs can contribute, the study also showed that HPs can not support as significantly as EVs can. On the other hand, the disadvantage with EVs is that they move, compared to the stationary HPs. The total HP capacity was 460 MW, and it was assumed that 46 MW were controllable. The EV inverter capacity was $\pm$ 90 MW with a battery capacity of 640 MWh. The necessity of a BESS with and without frequency support from HPs and EVs was also studied. It showed that utilizing HPs an EVs for frequency regulation could decrease the nescessary BESS size from 175 MW to 50 MW. The study concludes that if the investment in controlling HPs and EVs is smaller than the price of a 125 MW larger BESS, then using HPs and EVs for support is profitable. The HP model in this study is depicted on Figure 2.13 [12]. The model consists of LFC signal which can be controlled within $\pm$10% of the rated capacity, and a power consumption based on the energy demand. The start up of the HP is based on a ramp signal, and then it runs until enough water has been heated according to the energy demand. The time it takes to meet the demand is based on average values with a standard deviation, since the study considers several different demand profiles. Hence, a normal distribution is used stop the HP when the demand has been met [12].
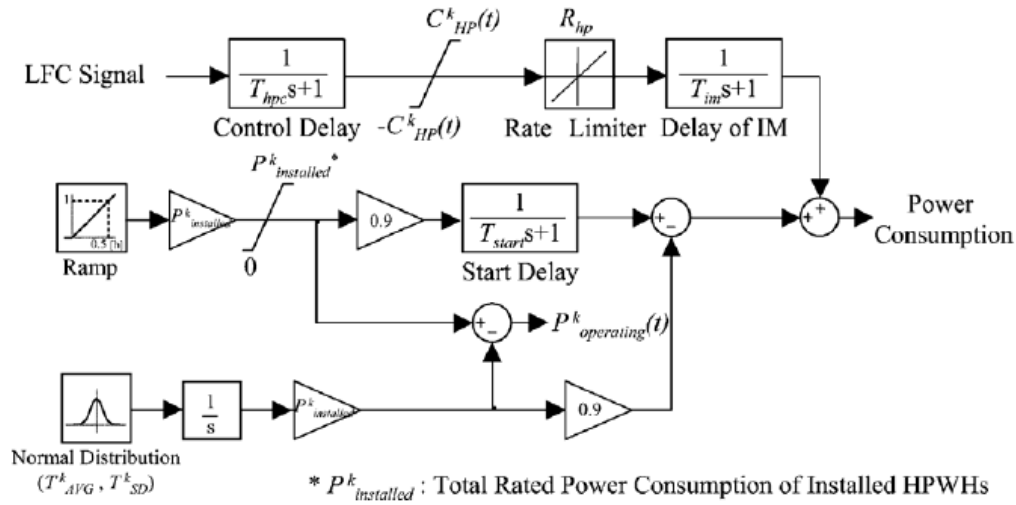
Figure 2.13: A HP model represented in [12].

Reference [29] studies how we wisely can control HPs for frequency regulation. A variable speed HP is considered. It focuses on a healthy control of the HP and the comfort of the customer, i.e. the customer's comfort should not be affected by the control. The controller is based a variable speed drive combined with a air temperature control. The study showed that the frequency response in a micro grid was improved by the controller proposed.

Some papers focus only on the modelling, some only on the frequency response with the use of a previously modelled HP, while others focus on both. In [19] the focus is mainly on the modelling part. Here a model for a HP and an electric boiler are developed and validated. The models are not used for anything further than validation in this paper.

A thorough investigation of future interactive energy system considering heating, transport and grid can be found in [31]. Two HP models are represented in this study. The first one is a quite simple model, with a storage tank that is controlled with a simple ON/OFF control based on the energy state of the tank. The energy state is calculated using the heat demand, the energy loss and the actual HP power. The second one is a more detailed model, which focuses on capturing the physical aspects of a HP. These two HP models are designed for analysis in distribution grids.

A review of HPs in power systems is represented in [32]. It presents the affects HPs can have on grids together with a financial and renewable aspect. The most frequently used controls of HP systems are represented. This paper does not develop or implement HP into grid application, but merely presents an overview.

Finally [33] focuses solely on how to control HPs for frequency regulations without affecting the customers comfort. A controller is represented, but no conclusions are made on the frequency is improvements by the controller.

As shown above there is a significant research interest on this topic. HP models were

developed in [12, 19, 29, 31] for differnet applications. Some focus on improving the grid frequency, while other focus more on the HP consumer. The model in [12] is considered to be the most relevant for this study, as this model is used together with a LFC.

2.4 Conclusion

This chapter started by introducing the chosen study case. The present electrical power system and heating sector were described, as well as some future plans were represented. The theory behind frequency regulation, especially primary and secondary frequency, was explained. The frequency requirements for the Faroe Islands were briefly introduced. Finally some examples of studies regarding the HPs possible contribution to frequency regulation were discussed. As the Faroese power grid will become increasingly renewable and the heating sector will be electrified, an investigation of the possible frequency regulation contribution by HPs is considered highly relevant. This study will focus on the an aggregated model of a HP, and how this can be controlled in order to contribute with frequency regulation with a developed LFC on the most southern island ('Su' on Figure 3.3) in the Faroe Islands.

Chapter 3

Study Case: Description and Modelling

It is a well known fact that a high penetration of wind power in a power system causes difficulties regarding frequency stability. As the shares of synchronous machines in power systems is decreasing, new methods to provide frequency regulation have to be implemented.

One of the researched methods is to use flexible loads like e.g. heat pumps or electric vehicles in load frequency control, this was discussed in chapter 2. This investigation uses heat pumps in a wind dominated power system to contribute to load frequency control.

Suðuroy, the most southern island in the Faroe Islands, is electrically isolated from the other islands. This island is the study case of this project. Currently the installed capacity is 19 % hydro and 81 % conventional, but in the transition to renewable energy this will change. A large part of the conventional power on Suðuroy will be replaced by wind power. The heating sector will be electrified, which makes the investigation of using heat pumps to contribute to frequency regulation on this island highly relevant.

This chapter describes the study case and explains the modelling of it. First a general introduction to the grid it self with installed capacities and production is presented. Then the DIgSILENT model of the grid is explained and tested. This includes loads, present generating units and future additions of wind power to the grid. The load frequency control and the heat pump implementation is explained in the next chapters.

3.1 The Grid on Suðuroy

There are two power plants on Suðuroy one hydro power plant (HPP) and one conventional power plant (CPP). The installed capacity currently consists of two hydro turbines rated at 1.3 MW and 2.6 MW, and four diesel generators rated at 2.56 MW, 2.56 MW, 4.18 MW

and 3,97 MW. The plan is to increase the capacity by installing WTs in the near future, see section 3.5.

3.1.1   Production on Suðuroy

Figure 3.1 shows the production throughout two months. (a) shows the production in a winter month, while (b) shows a summer month. The production is divided into the power produced at the HPP and the CPP. Additionally, the number of generating units online are shown.

The production varies significantly throughout a month. A possible explanation is a relatively large factory that is located on Suðuroy. When the factory is running it can consume up to the same amount of energy, as the rest of the island. Therefore, the production is increased quite significantly when the factory is running.

During the winter the hydro production is higher than during the summer, which is not surprising as the hydro production depends on the precipitation, and the basins are relatively small. The difference is not big however, and this can be explained by the relatively mild seasons.

Both during the summer and the winter the number of units online daily varies between 3 and 5 units, but generally there are more units online during the winter than in the summer. In the summer there are on average 4.0 units online, while the average during the winter is 4.3 units.
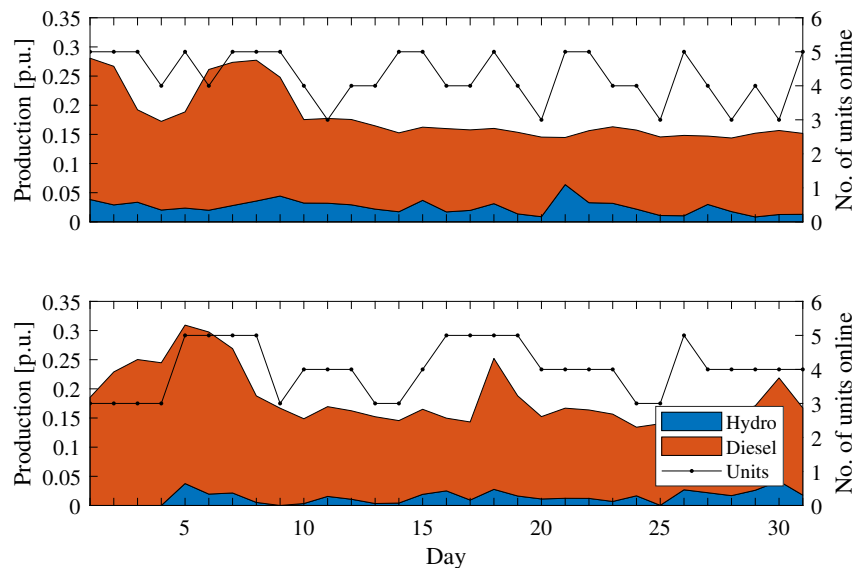
Figure 3.1: Production throughout two months. (a) A winter month and (b) a summer month.

The production for an average winter day, and an average summer day are shown in

Figure 3.2. These two average days, are based on the months shown in Figure 3.1. The production is shown in an hourly resolution. The production during the summer day is close to stable, while during the winter the production varies more. As in the previously shown figure, the production from the HPP is lower in the summer than in the winter, due to the climate.

Based on Figure 3.1 and Figure 3.2, it can be said that in general both plants are in service during the summer and in the winter. The shares of the production varies however.
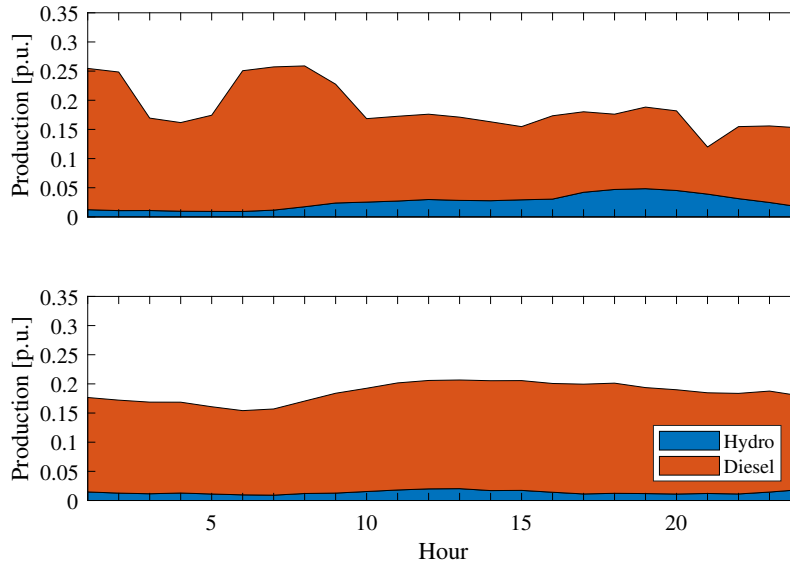
Figure 3.2: Production throughout two average days. (a) Average day in winter month, and (b) an average day in summer month.

3.2   The Model of the Grid

Dansk Energi, the non-commercial organisation for Danish energy companies, have developed a model of the Faroese grid in DIgSILENT for SEV. This model is the base of the model used for simulations in the present study. The model of the grid on Suðuroy is the only part of Dansk Energi's model that will be described in this section, as the investigation is focused on this island solely.

The grid model is shown in Figure 3.3. There are three voltage levels on Suðuroy, 20 kV, 10 kV and 0.4 kV. The transmission lines between the power plants are 20 kV, while the plants are 10 kV. The distribution lines between the villages on Suðuroy are 10 kV.

The model used in the simulations is; however, a simplified version of Dansk Energi's model. The modifications made to the model consist of aggregation of loads and production units.
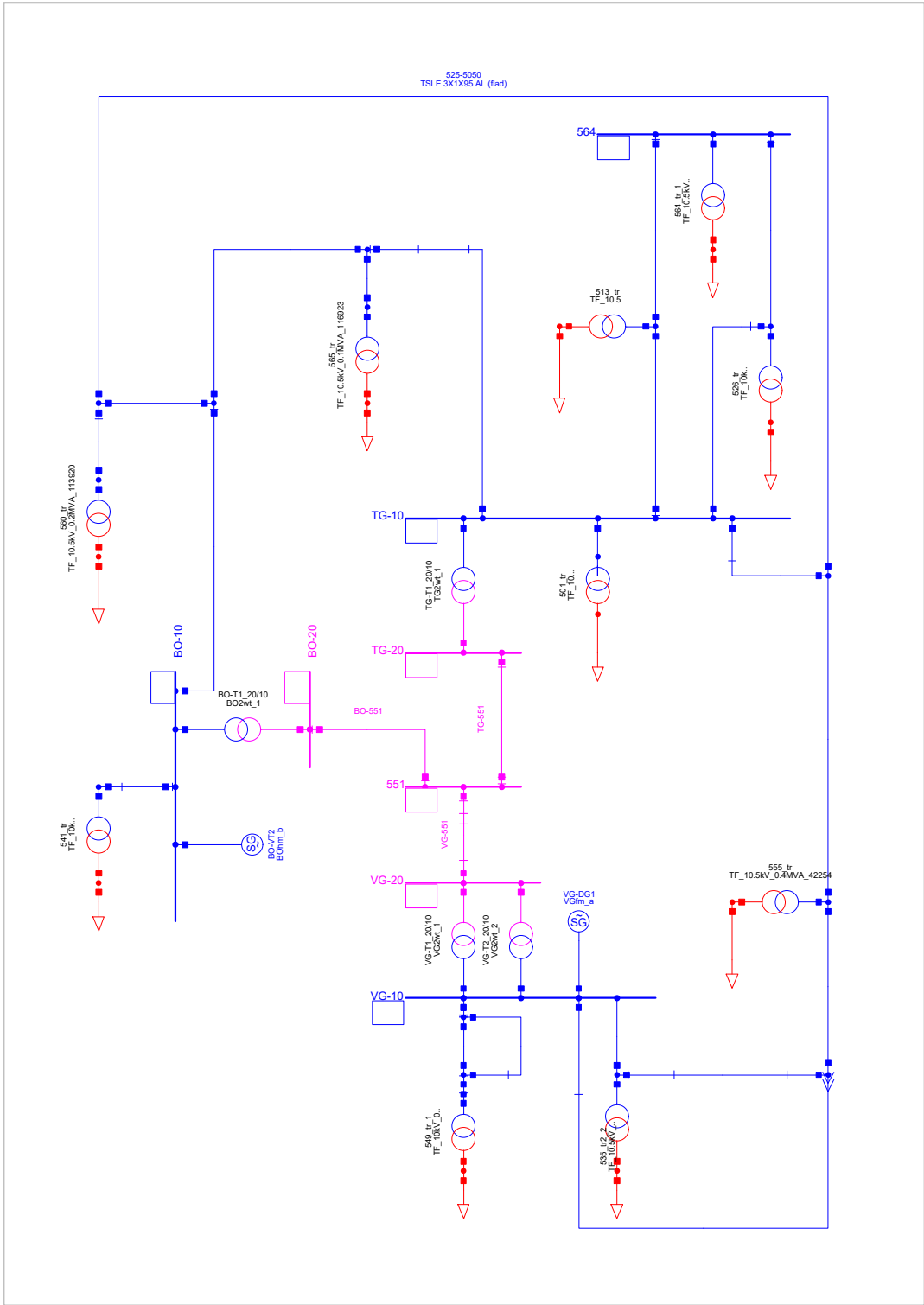
Figure 3.3: DIgSILENT layout grid. The voltage levels are 20 kV (pink), 10 kV (blue), and 0.4 kV (red).

The 4 diesel generators and 2 hydro turbines on Suðuroy, have been aggregated to one of each type. The conentional power plant (CPP) in this model is rated at 13.28 MW and the hydro power plant (HPP) is rated at 3.12 MW. In the original model there were 75 loads, while in the aggregated model there are 10 loads. The aggreagtion of the loads made it necessary to increase the size of the 10 kV/0.4 kV transformers in order to avoid over loading.

3.3 The Loads

There are 10 loads in the aggregated grid model. These loads, shown in Figure 3.3, are modelled as 100 % dynamic loads, which according to [34] can be represented by Equation 3.1. P_L and P_L0 are the load and the initial load, k_pf is the frequency dependant coefficient which is set to 0.2, k_put is the voltage dependency coefficient and set to 1. Finally, Δf and ΔU are the frequency and voltage deviations.

$$P_\mathrm{L} = P_\mathrm{L0}\big(1 + k_\mathrm{pf}\Delta f + k_\mathrm{put}\Delta U\big) \tag{3.1}$$

The measured load on Suðuroy has been obtained to use for simulations [35]. The data is from 2014. Figure 3.4 shows the total load (hourly based) on Suðuroy throughout a winter and summer day.

The two load profiles show a similar pattern during the winter day and the summer day, but load in the winter is slightly higher, which is likely due to an increase in e.g. lighting and heating. The load during the winter is between 2.5 MW and 4.2 MW, and between 1.9 MW and 3.5 MW during the summer day.
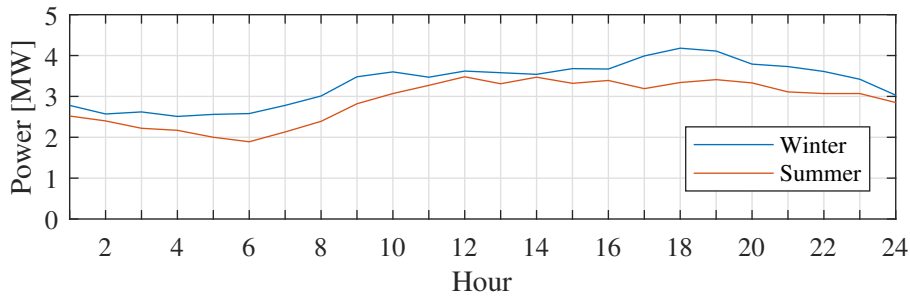
Figure 3.4: The total load on Suðuroy during a winter day (blue) and a summer day (red).

Each of the 10 loads is set to be loaded by 10 % of the total load during the simulations of the grid. The measured load is sent to the loads in the model using a measurement file (`.ElmFile`).

3.4   Diesel and Hydro Units

The generating units on Figure 3.3 are equipped with a governor and an automatic voltage regulator (AVR). Figure 3.5 [36] shows a simple diagram of a generator with a governor and an AVR. The working principle of a governor was explained in chapter 2. The AVR controls the voltage, as the name implies. The output voltage is detected and compared with reference voltage. If the output voltage differs from the reference voltage, the voltage is regulated accordingly by adjusting the field current [37].
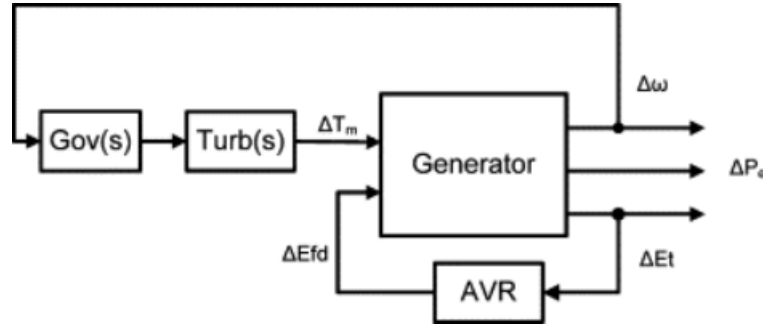
Figure 3.5: Schematic diagram of generator with AVR and a governor. [36]

The governor and AVR are modelled in DIgSILENT using standard models from the library. A hydro turbine governor is used for the HPP, and a thermal governor is used for the CPP. Both plants are modelled with the same AVR model. The block diagrams of the models, together with the used parameters can be found in Appendix A.

3.4.1   Governor Repsonses

The response of the governors to a power deficit has been calculated and simulated. The steady state frequency deficit due to a power change can be calculated using the nominal frequency and power, the droop and the power deficit.

First, the frequency characteristics, β [MW/Hz] is calculated using Equation 3.2, where P_n and f_n are the nominal power and frequency and R is the droop [38].

$$\beta = \frac{P_n}{R \cdot f_n} \tag{3.2}$$

In a system with more than one droop controlled machine, the frequency characteristics are added together. When β is known, the steady state frequency can be calculated using where ΔP represents the power deficit [38].

$$f_{ss} = f_n - \frac{\Delta P}{\beta} \tag{3.3}$$

The droop and the frequency characteristics of the HPP and the CPP are summarized in Table 3.1.

	Droop Constant R	Frequency Characteristics β [MW/Hz]
HPP	0.04	1.56
CPP	0.047	5.65
Total β	-	7.21

Table 3.1: The Droop and Frequency Characteristics of the HPP and CPP.

The frequency response has been with each plant seperately and together. The power set point of the CPP is set at 6.64 MW, and the HPP is set at the same proportionality to its size, i.e. 1.56 MW. The load is set at 6.64 MW in total when testing the CPP, and 1.56 MW when testing the HPP. In the case where both plants are online, the load is set at 8.2 MW. The simulation is conducted with a total load increase of 10 % at 5 seconds.

Figure 3.6 shows the frequency and power response to the power deficit when the units are tested separately. The response of the HPP is a smooth response. When the load is increased the frequency drops below 49.1 Hz after five seconds. The frequency then slowly rises up to 49.91 Hz where it stabilizes 25 seconds after the deficit. The power response to the contingency is an increase of 0.05 p.u.

The increased load impacts the frequency differently when the CPP is online, than when the HPP was online. The frequency does not drop as significantly as before, but now it oscillates on the contrary to the HPP response. The frequency stabilizes at 49.88 Hz at 20 seconds. The power increases with approximately 0.05 p.u. similarly to the HPP response.
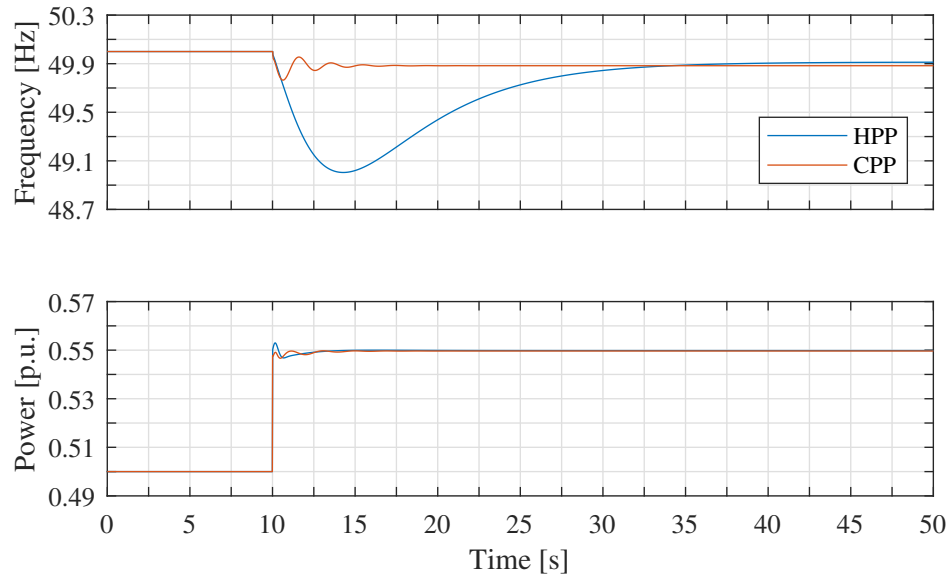
Figure 3.6: Frequency and power response to load event, generators tested separately.

With both plants online, the frequency response is a mixture of the two first ones, this is shown on Figure 3.7. There are some oscillations visible at the beginning as there were with the CPP test, and the frequency increases slowly back to 49.89 Hz after 200 seconds. The power of the CPP increases fast by 0.06 p.u. and then decreases back to 0.55 p.u., while the HPP power increases slowly to 0.56 p.u. The oscillations and how fast the response is, depends on the time constants of the machine controls.
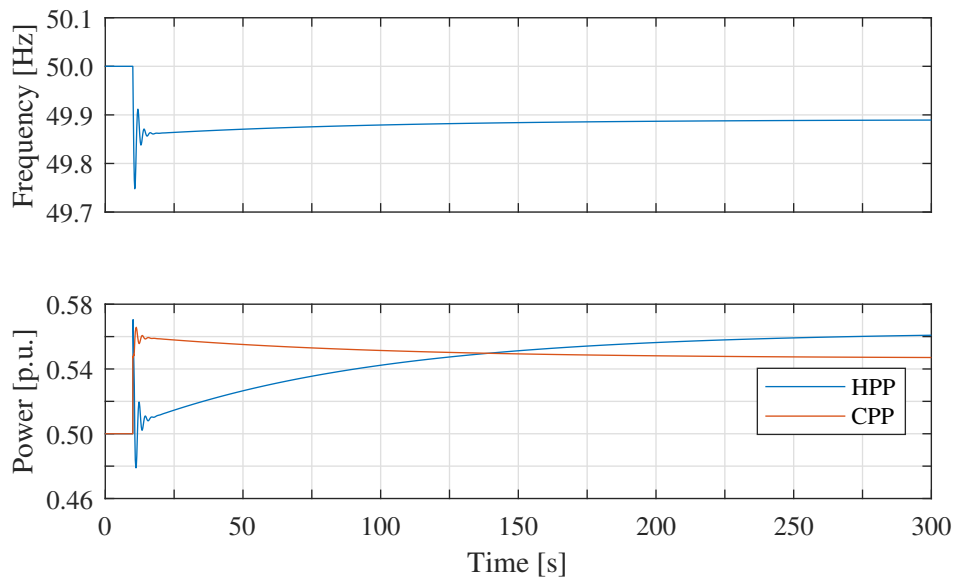
Figure 3.7: Frequency and power response to load event, generators tested together.

The calculation and simulation results are summarized in Table 3.2. The CPP and HPP+CPP results are identical while there is a 0.01 Hz difference for the HPP, this is not considered as a significant difference.

	Calculation	Simulation
HPP	49.90	49.91
CPP	49.88	49.88
HPP+CPP	49.89	49.89

Table 3.2: Calculated and simulated steady state frequency.

3.4.2 Generator Responses with Rate Limiter

The governors in DIgSILENT give a fast response with a high rate. In reality there are however some mechanical and thermal constraints [39]. To account for this a rate limit with a time delay has been added between the LFC control, explained in subsection 2.3.1, and the governors.

Figure 3.8 shows how the rate limit has been built. The input, p_{lfc}, is delayed by the time delay, τ_r, and limited by the respective limit. The output, p_{gov} is sent to the governor as a set point, that will increase or decrease the turbine power according to the input signal.
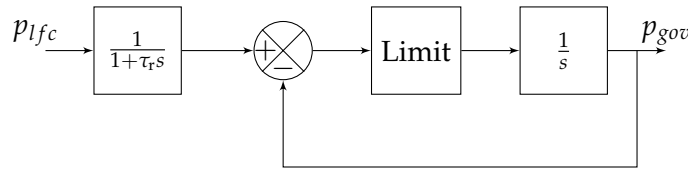
Figure 3.8: The rate limiter.

According to Danish TSO Energinet.dk's technical regulations, the power ramp rate of a diesel power plant over 1.5 MW should be 20 %/min [39]. Energinet.dk's technical regulations does not contain ramp rates for HPPs, and in the Faroe Islands there are no official requirements for ramp rates, hence the hydro ramp rate is assumed to be 10 %/min. The time delay was assumed to be 4 seconds.

The rate limiter has been added to the model and tested, the results are shown in Figure 3.9. The input to the rate limiter was increased by 0.1 p.u., and as the figure shows the output power of the generators increases by 0.1 p.u accordingly. The repsonse of the HPP is slower than the CPP, which corresponds to the ramp rates. The CPP power can increase by 20 %/min, while the HPP can only be increased by 10 %/min.
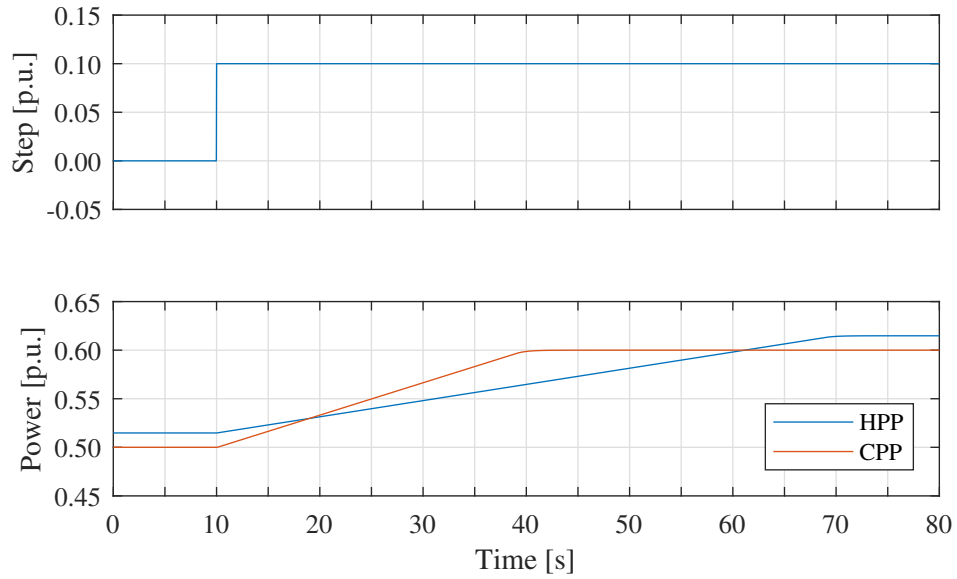
Figure 3.9: Response to step signal through rate limiter.

3.5   Wind Power

The majority of the power currently produced by fossil fuels, will be replaced by wind power, in the transition towards a 100 % renewable power system. More precisely, two wind farms of maximum 6 MW will be installed. The first was to be installed in 2018, and the other one in 2020, but this project has however been delayed. There is a possibility that all 12 MW will be installed in 2019 [40].

The power produced by a wind turbine (WT), P_{WT}, is calculated following Equation 3.4 [41]. The air density is noted by $\rho\,[\text{kg/m}^3]$, $A_R\,[\text{m}^2]$ is the swept area of the rotor, $v\,[\text{m/s}]$ is the wind speed and C_P is the power coefficient. The power coefficient is defined as the efficiency of the rotor [41].

$$P_{WT} = \frac{1}{2} \cdot \rho \cdot A_R \cdot v^3 \cdot C_P \tag{3.4}$$

In this investigation two WFs of 5.4 MW, that consist of six ENERCON E-44 WTs rated at 0.9 MW, are assumed to be installed. This WT type has previously been identified as the best suited WT for Faroese conditions [42].

The characteristics of a Enercon E-44 WT, in terms of the produced power and the power coefficient as functions of the wind speed, are shown in Figure 3.10 [43]. The WTs are equipped wth a storm control with a cut-out wind speed between 28 m/s and 34 m/s; however, the official power curve is given for wind speeds from 1 m/s to 25 m/s, and therefore the production at wind speeds above 25 m/s is set to zero for this study. The figure shows that the power output reaches its nominal value for wind speeds above 15

m/s, and that the highest power coefficient is between 8 m/s to 10 m/s.
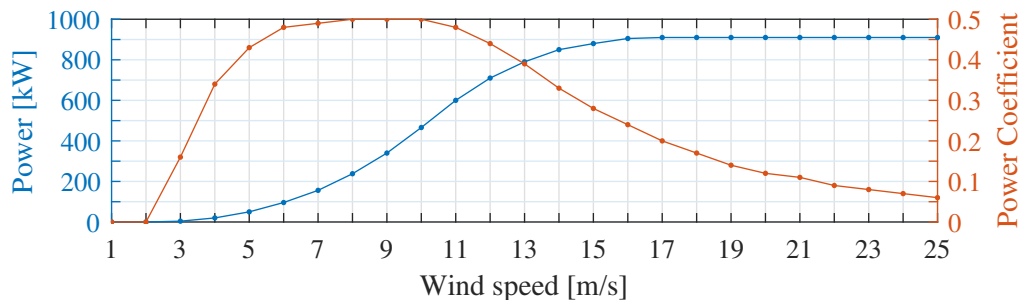
Figure 3.10: The characteristics of a ENERCON E-44 WT. The blue line is the power curve, while the red line illustrates the power coefficient [43].

3.5.1 Potential Production from Wind Farms

Figure 3.11 shows the calculated potential production from a 5.4 MW WF for a winter day, together with the wind speed. The wind speed used for calculations is measured values from the Faroe Islands. The high wind speeds this day result in no production over approximately 4 hours of the day, and a total potential production of 96 MWh.
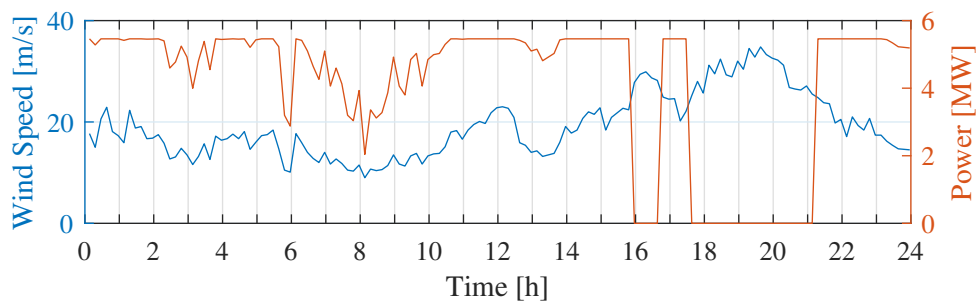
Figure 3.11: Potential production (blue) from a 5.4 MW WF during a winter day with the measured wind speed (red).

Similarly to the winter day, the potential production has been calculated for a summer day, see Figure 3.12. The total production for this day is 12 MWh, which is approximately 12.5 % of the production during the winter day.
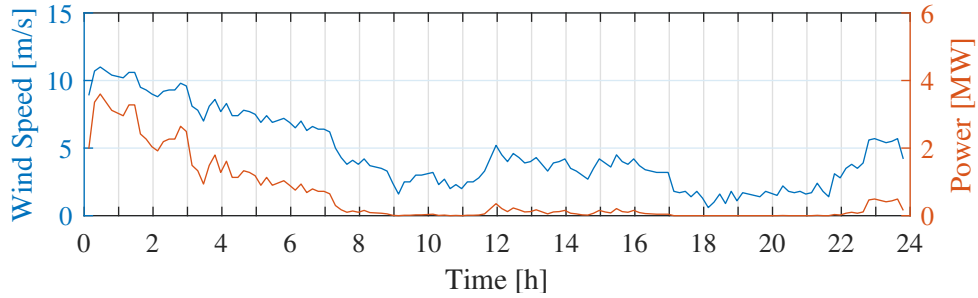
Figure 3.12: Potential production (blue) from a 5.4 MW WF during a summer day with the measured wind speed (red).

An interesting observation is that the potential production from one WF during the winter actually exceeds the measured load shown in Figure 3.4 for a large part of the day. This will, in practical application, result in the necessity to curtail the WTs in order to obtain a balanced production. If two WFs of six E-44 WTs are installed on Suðuroy, the potential production is 10.8 MW, which is two to three times the load measured in 2014. How this is handled in the simulations is explained in section 4.3.

3.5.2   Modelling of Wind Farms

Each WF is represented by a constant power static generator (`.ElmGenstat`) in the DIgSI-LENT model. The static generators are connected to the VG-10 busbar, which is the lowest busbar on Figure 3.3. This 10 kV busbar is the 10 kV busbar in the model that located closest to were the wind farms are planned. A measurement file with the potential production is used to set the active power of the static generator.

3.6   Conclusion

This chapter has explained the study case and the modelling of it. First the grid it self was explained, and production data were presented. The loads with a load profile were then introduced. Next the current production units, the diesel and hydro units, were discussed. These were tested both based on the primary response of a governor and with a rate limit added before the governor. Finally, the wind power added to the grid for considerations of future scenarios was represented with the potential production. All models have been tested and validated.

Chapter 4

Load Frequency Controller

The purpose of a load frequency controller is to maintain a balance between the loads and the generation. A perfect balance is impossible, as the responses of controllers, generators and loads are not instant, but with a carefully designed controller the frequency can be improved significantly.

This chapter explains the designed LFC controller and the strategy behind it. The controller is tested, and the different test scenarios are explained. Assumptions made on the load profile and the wind power are described, and finally simulation results for different test scenarios with the LFC implemented are represented.

4.1   The Designed Controller

The LFC is designed to give a secondary frequency response with the CPP, the HPP and the HP. Specifics about the HP are discussed in the following chapter. The power balance with this power system can be obtained by Equation 4.1. When $\Delta P \neq 0$ the frequency will deviate from the nominal frequency. A positive ΔP means that there is an overproduction, which results in an increased frequency. The deviation will be detected by the primary control of the HPP and the CPP, and the LFC of the HPP, CPP and HP and the frequency will be corrected accordingly.

$$\Delta P = P_{\mathrm{CPP}} + P_{\mathrm{HPP}} + P_{\mathrm{WT}} - P_{\mathrm{HP}} - P_{\mathrm{L}} \tag{4.1}$$

The LFC is designed as shown in Figure 4.1. When a frequency deviation is detected the input signal, that is in p.u. will be multiplied with the nominal frequency to obtain the frequency deviation in Hz. This is signal is passed to the frequency bias factor, B [MW/Hz], which is the summation of the frequency characteristics of the system [38]. The next block is a PI controller, which then sends the signal to the dispatch block. The dispatch block decides how much each LFC controlled unit has to be regulated to correct

33

the error, and p_{lfc} is sent to its respective units. The amount sent to each unit is set by a LFC participation factor. The parameters of the LFC controller can be found in Appendix B.
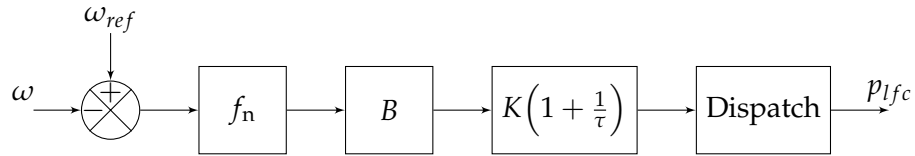
Figure 4.1: LFC block diagram.

4.1.1 Test of LFC

The LFC has been tested to a power deficit with LFC participation from the HPP and CPP. The results are shown in Figure 4.2. (a) shows the frequency response and (b) shows the respective regulation power of the two plants. It can be seen that the frequency settles back to 50 Hz after some time, and the controller therefore works as desired.
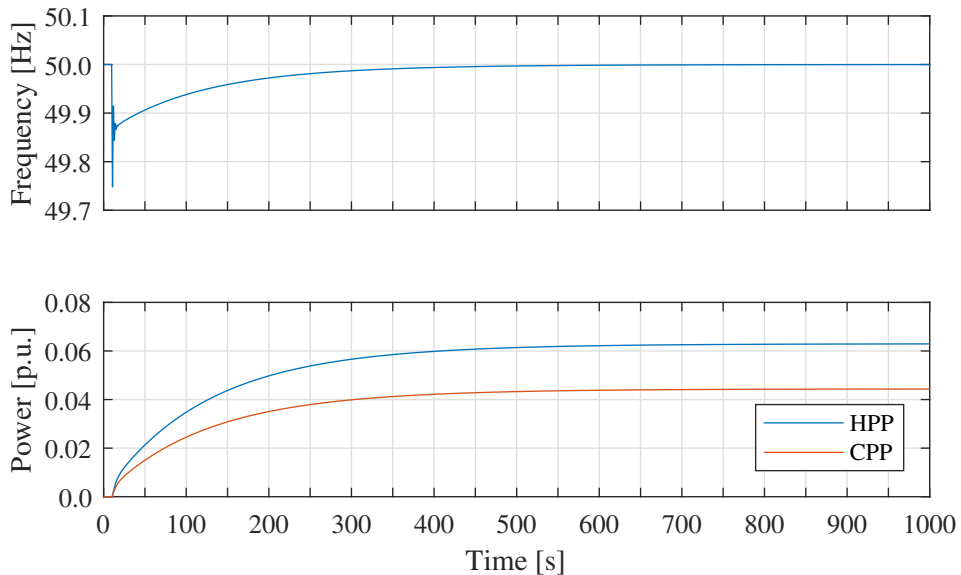
Figure 4.2: Frequency response and regulation power for test of LFC with HPP and CPP.

4.2 Load Assumptions

The load on the Faroe Islands has historically increased by 2 % annually [4]. Since the load profile obtained is from 2014, the load is projected using a 2 % annual increase from 2014 to 2018 and to 2020 for the simulations with one and two WFs, respectively.

In addition to an annual load increase, the base load of the heat pumps is added to the load profile, see section 5.2 for further specifications.

4.3 Wind Power Adjustment

It was briefly mentioned in section 3.5 that the potential production from the planned wind farms, actually exceeds the total load on Suðuroy quite significantly.

Therefore, there is a necessity to keep some WTs offline. How many WTs are online was decided using the following strategy; the total load is divided by the potential wind production from one turbine, this number is then rounded and it was assumed that the system can handle the number obtained.

Simulations showed that the assumption above was wrong, and the number of WTs had to be reduced even further for some of the simulated scenarios. This was done using a trial/error procedure. This process showed that the grid on Suðuroy is very fragile, and a fluctuation in wind power production of 0.5 MW is enough to stop the model from converging in some scenarios.

4.4 Simulation Results

The LFC of the CPP and HPP is tested based on the following six scenarios:

1. Current generating units - The winter day load from 2014.
2. Current generating units - The summer day load from 2014.
3. 1 WF added - The winter day load projected to 2018 with heat pump base load.
4. 1 WF added - The summer day load projected to 2018 with heat pump base load.
5. 2 WFs added - The winter day load projected to 2020 with heat pump base load.
6. 2 WFs added - The summer day load projected to 2020 with heat pump base load.

The results are first represented by figures, and then summarized a table at the end of the chapter with the minimum, maximum and average frequency together with the LFC participation factors and the wind shares.

4.4.1 Current Scenario: Winter

Figure 4.3 and Figure 4.4 show the simulation results based on the current scenario with the HPP and the CPP and the load profile presented earlier. The frequency (a) and the power production and consumption (b).

There are frequency spikes every hour, because the load profile is hourly based. A load profile with a higher resolution would increase the amount of frequency deviations. The minimum frequency reached is 49.9 Hz, while the highest is 50.08 Hz for the winter scenario. Overall, the frequency deviations are small, considering that the frequency requirements of normal operation of the Faroese grid are that it should be between 49.5 Hz and 50.5 Hz [28], and instantaneous values can be even lower as explained in chapter 2. The LFC participation factor for each unit is assumed to be proportional to the size compared to the total capacity, hence is set to 19 % by the HPP and 81 % by the CPP.
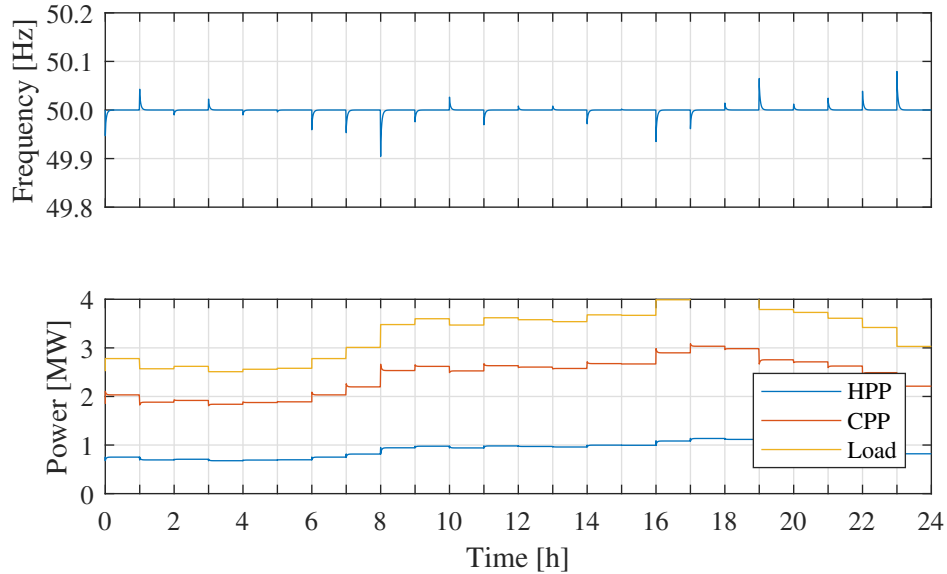
Figure 4.3: LFC winter with base load 2014. (a) Frequency and (b) the power production and consumption.

4.4.2 Current Scenario: Summer

The frequency response during the summer is quite similar to the winter scenario. There are some frequency spikes, but the frequency is restored to 50 within a reasonable time. The minimum frequency reached with summer scenario is 49.87 Hz, and the maximum is 50.07 Hz. The participation factors in the summer are the same as in the winter.
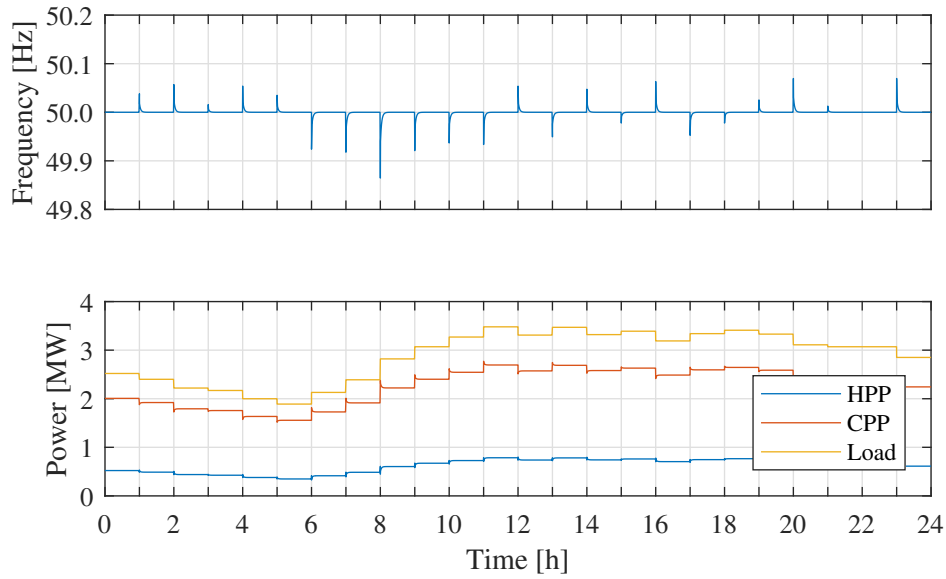
Figure 4.4: LFC summer with base load 2014. (a) Frequency and (b) the power production and consumption.

4.4.3 With 5.4 MW WF: Winter

As a 5.4 WF is added to the system, the CPP capacity is decreased by 2.56 MW, this is the rating of one of the diesel generators installed on Suðuroy. The participation factor of the LFC has been adjusted accordingly, see Appendix B.

The frequency during a winter day with a 5.4 MW WF added to the system is shown on Figure 4.5. Compared to Figure 4.3 the frequency fluctuations are more obvious now, and this is due to the added production from the WF which fluctuates. The frequency now varies between <49.5 Hz and >50.3 Hz, compared to 49.87 Hz and 50.07 Hz.
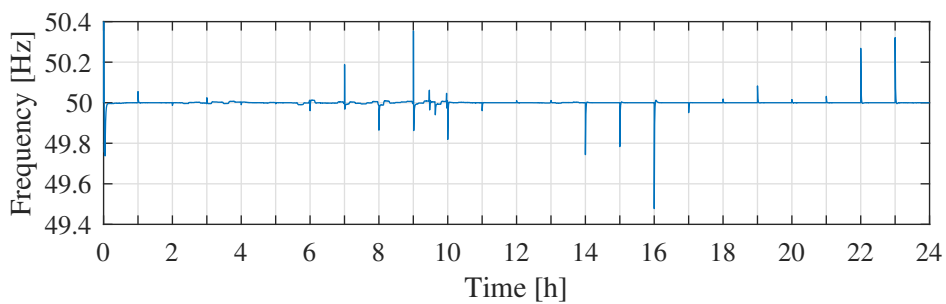
Figure 4.5: Frequency response - winter day with one WF.

Figure 4.6 shows the power output of the two plants. The HPP reaches a maximum output of 0.5 p.u. while the highest production by the CPP is 0.3 p.u. It can seen that the power

from hour 0 to 14 fluctuates more than during the rest of the day, this is caused by the fact that the WF shuts down from hour 16 to hour 22 due to too high wind speeds, and the CPP and HPP therefore only regulate according to the hourly based load during this time.
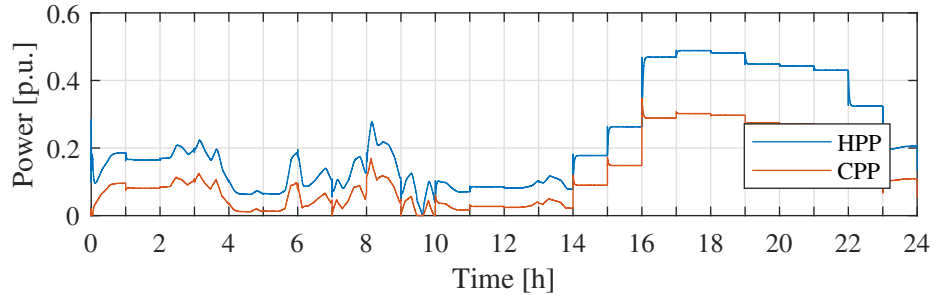
Figure 4.6: Power output of CPP and HPP - winter day with one WF.

The wind production is shown on Figure 4.7 which covers 50 % of the total production, that reaches a maximum production at 4 MW. The production is lower than the potential production due to previously explained reasons.
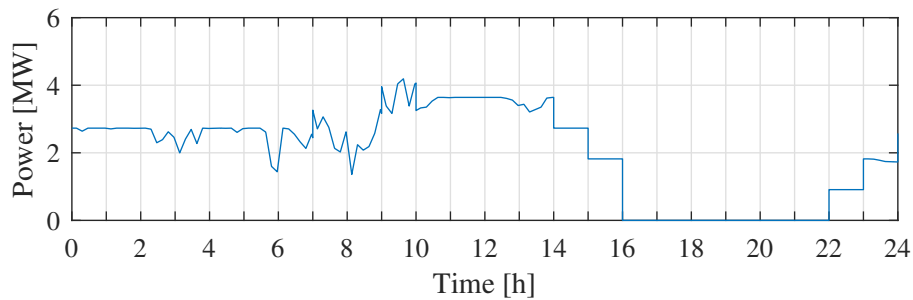
Figure 4.7: Wind power production - winter day with one WF.

4.4.4   With 5.4 MW WF: Summer

The frequency during the summer day with one WF installed, Figure 4.8, fluctuates quite significantly during the first six hours, and this is explained by the high share of wind power, which can be seen on Figure 4.10. All six WTs are online throughout the day, and for the first hours the WTs are dominating the production.
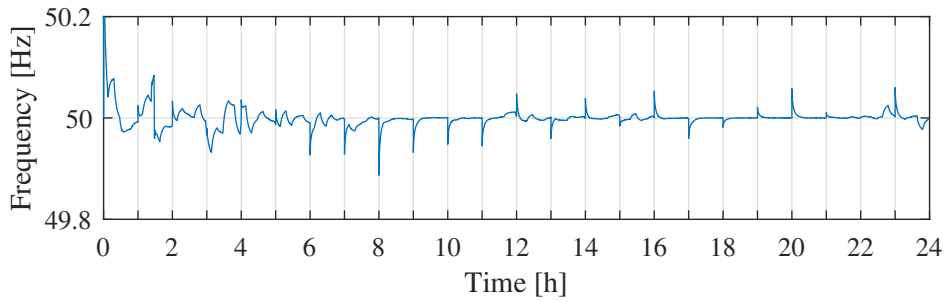
Figure 4.8: Frequency response - summer day with one WF.

Since the WF covers a large part of the production during the first few hours, the power of the HPP and CPP is quite low, see Figure 4.9, but as soon as the production from the WF decreases, the production from the CPP and HPP increases. The wind share is 18 % in this scenario.
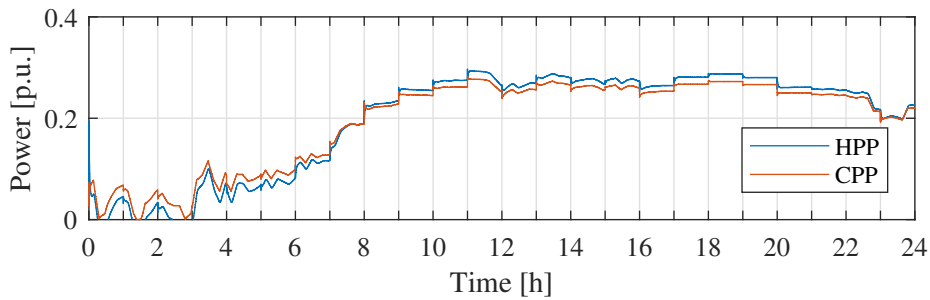
Figure 4.9: Power output of CPP and HPP - summer day with one WF.
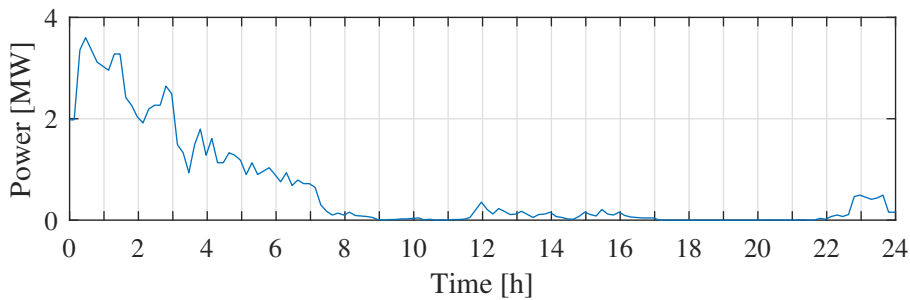
Figure 4.10: Wind power production - summer day with one WF.

4.4.5 With 10.8 MW WF: Winter

Another 5.4 MW WF has been added to the system, and conventional capacity has been decreased by 2.56 additional MW. The LFC participation factor has been changed as well. The frequency during the winter with a 10.8 MW WF is quite similar to the frequency with

a 5.4 MW WF. This is because the number of WTs online throughout the day is almost identical.
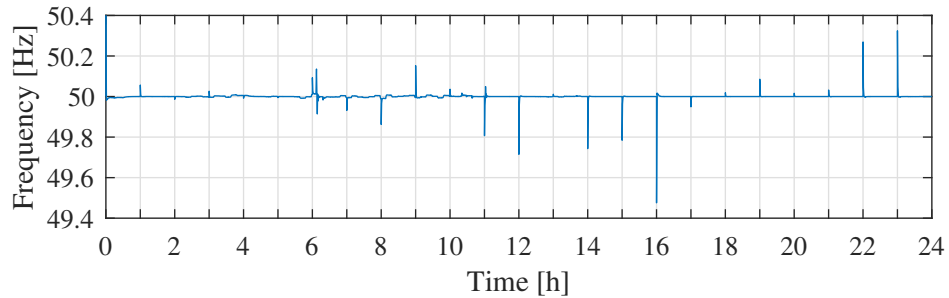
Figure 4.11: Frequency response - winter day with two WFs.

The power output of the CPP and HPP during a winter day with two WFs is shown on Figure 4.12. It shows a behavior similar to Figure 5.7, but with a higher generation, since the load has been increased, and the WF production is close to the same as before.
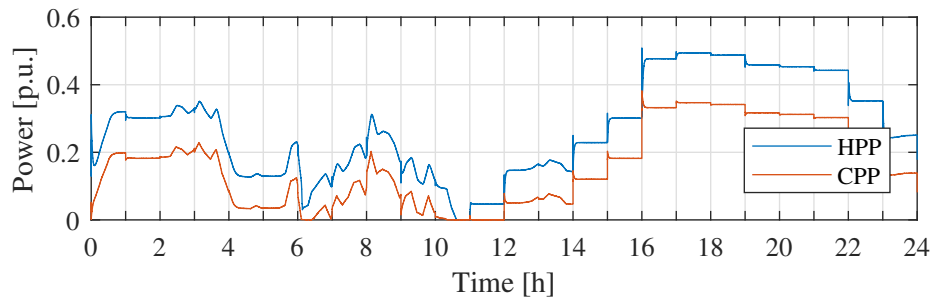
Figure 4.12: Power output of CPP and HPP - winter day with two WFs.

By looking at Figure 4.13 and comparing it to Figure 4.7 the previous statement is verified; the wind production is almost the same. The reason is that the load is so low compared to the potential production that even though six WTs have been added to the system, they can not all be in service. The production is increased by 1 WT during hour 10 and 11, but that is the only difference. The wind shares with a 10.8 MW WF during a winter day are 45 %, which is actually lower than the share with a 5.4 MW WF, but again this is due to the increased load and a wind power production that is barely increased.
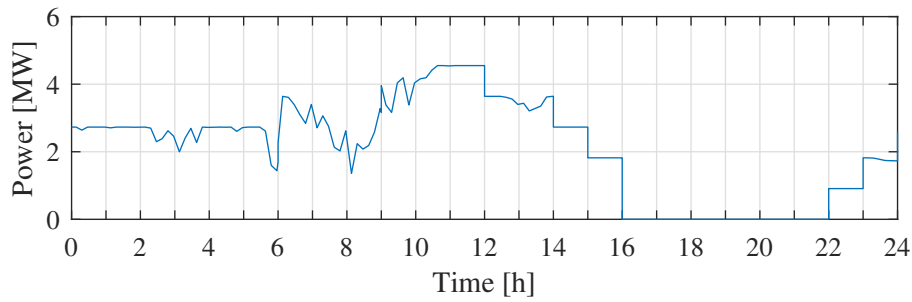
Figure 4.13: Wind power production - winter day with two WFs.

4.4.6 With 10.8 MW WF: Summer

Figure 4.14 shows the frequency during a summer day with two WFs installed. The frequency variates between 49.9 Hz and 50.18 Hz. In Figure 4.15 it can be seen that the output power of the plants is regulated according to the wind production shown in Figure 4.16.
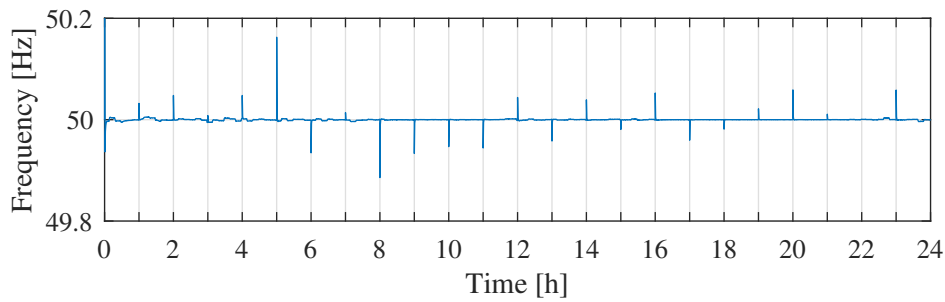
Figure 4.14: Frequency response - summer day with two WFs.

The power produced by the HPP and CPP is higher with the 10.8 MW WF than with the 5.4 MW, but this is due to the increased load, and the fact that the installed wind capacity does not increase the production significantly due to limitations and wind speed.
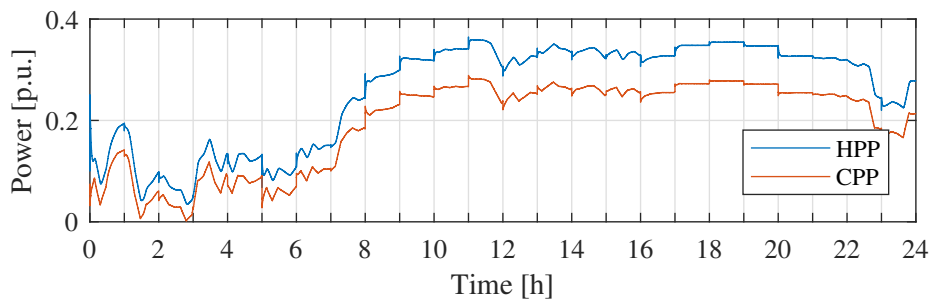
Figure 4.15: Power output of CPP and HPP - summer day with two WFs.

The wind speed during the summer is significantly lower than in the winter, therefore more WTs can be in service. There are limitations set on the first few hours, but otherwise all 12 WTs are online from hour 8 to hour 24, but the production never reaches 1 MW over this period due to the low wind speed. The wind shares have increased from 18 % to 19 % by having 10.8 MW installed instead of 5.4 MW.
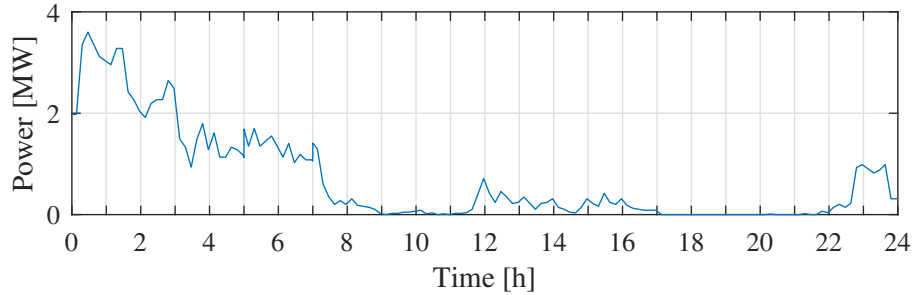
Figure 4.16: Wind power production - summer day with two WFs.

Table 4.1 summarizes the simulation results including minimum, maximum and average frequencies together with the LFC participation factor for the HPP and the CPP, and the wind power production.The average frequency was found to be 49.99 Hz for all six scenarios, the minimum and the maximum frequencies and the wind share vary depending on the scenario.

Scenario	HPP factor	CPP factor	Season	Wind Share	f_{min}	f_{max}	f_{avg}
Current	0.19	0.81	Winter	-	49.90	50.08	49.99
			Summer	-	49.86	50.07	49.99
1 WF	0.23	0.77	Winter	50 %	49.47	50.35	49.99
			Summer	18 %	49.89	50.08	49.99
2 WF	0.28	0.72	Winter	45 %	49.48	50.32	49.99
			Summer	19 %	49.89	50.16	49.99

Table 4.1: Simulations results summarized.

4.5   Conclusion

This chapter has shown that the implemented LFC is capable of restoring the frequency to 50 Hz. Without the WF the frequency deviations are small, but as more WF are installed the frequency deviates more. The frequency does however not vary very significantly compared to limitations of the grid code. The wind power shares vary between 18 % and 50 %

Chapter 5

Frequency Regulation with Heat Pump

This chapter is focuses on the frequency regulation provided by heat pumps. First the heat demand now, and the demand used in simulation is described, and then the heat pump model used is explained and tested. Finally the simulation results with frequency regulation contribution from heat pumps are represented and discussed.

5.1   Heat Demand

The heat demand used in the simulations is based on the data from [18] that was presented in chapter 2. Data for a winter day and a summer day have been obtained, and later sized for the appropriate scenario. The daily heat demand for one HP is shown in Table 5.1. The heat demand during the winter day is 89.2 kWh and in the summer day 28.5 kWh, which means that the heat demand is three times as big in the winter compared to the summer.

	Energy Demand E_d [kWh]
Winter	89.2
Summer	28.5

Table 5.1: The daily energy demand during a winter day and a summer day for one heat pump. 89.2 kWh are required in the winter and 28.5 kWh in the summer

In chapter 2 the coefficient of performance (COP) was briefly mentioned, and it was stated a that typical COP value is between 3 and 5. The COP varies according to the outside temperature and on the actual HP system. An example of the COP value relative to the atmospheric temperature, can be found in a [44], which is the datasheet for a HP. It can be approximated with Equation 5.1, where T_{atm} is the atmospheric temperature.

$$COP = -1.6 \times 10^{-5} \cdot T_{\text{atm}}^3 + 5.2 \times 10^{-4} \cdot T_{\text{atm}}^2 + 7.3 \times 10^{-2} \cdot T_{\text{atm}} + 3.4 \qquad (5.1)$$

Figure 5.1 shows the calculated COP based on Equation 5.1 and the outside temperature. The winter day and the summer day are shown. The COP in the summer is between 3.95 and 4.15. During the winter day the COP varies between 3.45 and 3.7. It can therefore be stated that the COP is generally lower in the winter than in the summer, which is consistent with the fact that temperature is higher in the summer than in the winter.
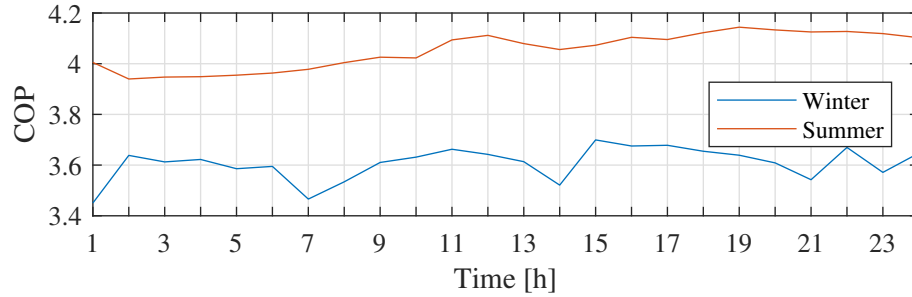
Figure 5.1: The hourly coefficient of performance during the summer and the winter day.

The average value of the COP in Figure 5.1 is presented in Table 5.2. In the summer the average is 3.61 and in the winter it is 4.05. The COP is often assumed to be constant in studies, but as it can be seen it varies quite significantly. Therefore two different average values have been used for the winter and summer simulations. How the COP is used in the model is explained in section 5.2.

	Average COP
Winter	3.61
Summer	4.05

Table 5.2: The daily average COP.

5.1.1   Heat Demand used in Simulations

There are approximately 1700 houses on Suðuroy [17], of which most use oil burners for heating. However, according to the 2030 vision, all of these will have transition to renewable solutions. If every house on Suðuroy was to install 6 kW HPs, it would results in a total capacity of 10 MW.

This report considers two stages of HP integration. For the scenario with 1 WF installed, it is assumed that 20 % of the houses or 425 houses have switched to HPs. The total rated capacity, based on 6 kW HPs, is 2.55 MW. The total energy demand is set to 37.92 MWh and 12.11 MWh in the winter and the summer, respectively.

In the second scenario with 2 WFs, the number of HPs is doubled to 850. This results in a total energy demand of 75.84 MWh in the winter and 24.22 MWh in the summer. The total installed capacity is now 5.1 MW. The values are tabulated in Table 5.3.

Scenario	Heat Pumps N	Rated Power P [MW]	Season	Energy Demand E_d [MWh]
1 WF	425	2.55	Winter	37.92
			Summer	12.11
2 WF	850	5.10	Winter	75.84
			Summer	24.22

Table 5.3: The heat demand, rated power and number of houses with heat pumps for the two tested scenarios.

5.2 Heat Pump Model

A HP model has been developed in order to implement the HP in the PowerFactory grid. The HP model is based on the previous research done in [12], which was discussed in chapter 2. The model has however been modified so that it could be applied to the researched scenario. The model is an aggregated model representing all the HP in the grid.

Reference [12] represents a model with a LFC signal and power consumed by the storage tank. The power consumption is based on a ramp function, and a normal distribution based on different types of houses. In this thesis only one demand profile is considered, therefore the model with a normal distribution can not be applied directly to this investigation. In [11] a base load has been added to the model in [12], to make the model more realistic. This has also been added in this investigation.

Figure 5.2 shows the model used in the investigation. A LFC signal is subtracted from the two other signals, which are the power demand from the storage and the base load. The summation of this is limited between a minimum and maximum. The minimum is set 5 %, as it is assumed that there will always be a need for a base consumption, which the LFC signal can not regulate the total consumption below. The maximum limit is the rated capacity of the HP system. The output signal is sent to the HP load. Each part of the model is explained in more details in the following subsections. The parameters of the models can be found in Appendix C.
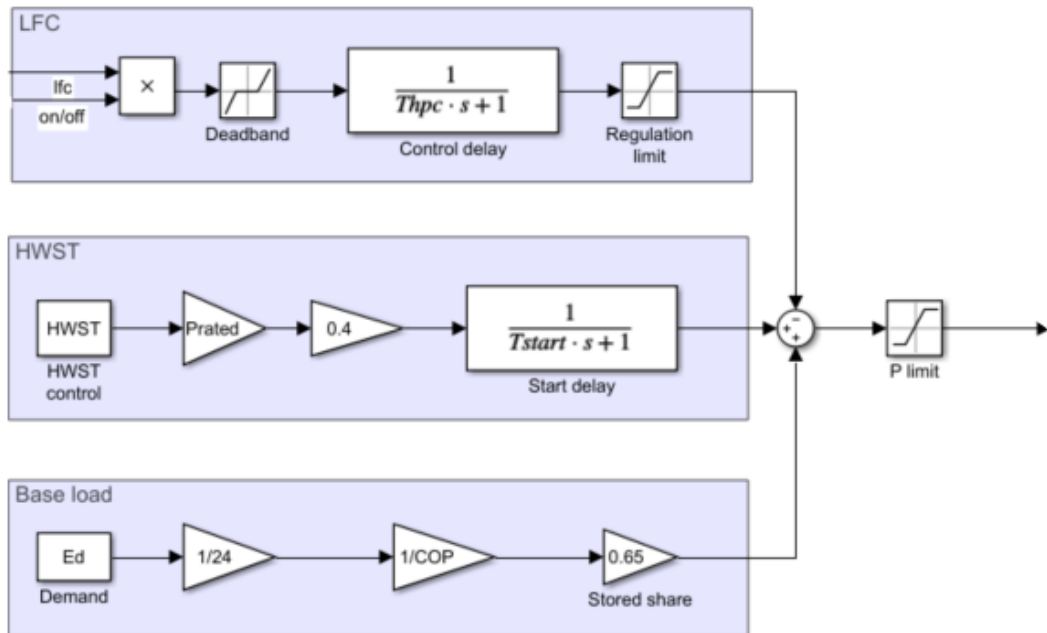
Figure 5.2: The heat pump model.

5.2.1 Load Frequency Signal

The LFC signal sent to the model is in MW, and if this value above the dead band set, it is used to control the HP. A dead band is added to avoid unnecessary use of the HP system. This dead band is also a requirement for demand side management as stated in chapter 2. A control delay has been added to account for delays in practical applications. It is assumed that the transmission system operator is allowed to regulate $\pm 40\%$ of the total capacity. The regulating capacity limit is set, for consideration of the comfort of the consumer. The signal is subtracted from the power consumption in order to provide the right response. The LFC signal is positive when there is an lack of energy. If the HP has to contribute for a scenario like this, the HP load has to be decreased, therefore the signal is subtracted from the total power.

The HP is limited to not provide LFC support for the first 30 minutes, which is the time when the power representing the storage reaches nominal power. This is done by sending a ON/OFF signal that is multiplied with the input LFC signal. Before 30 minutes the ON/OFF signal is 0, and after it is 1.

5.2.2 Storage Tank

The hot water storage tank (HWST) is used for 35 % of the total energy demand, which is stored at 40 % of the rated capacity. The rest, 60 %, is reserved for frequency regulation.

The power consumption of the storage is assumed to start at hour 0. It then it heats the water until it has reached what corresponds to 35 % of the energy demand. This is used to avoid hot water shortages throughout the day.

The time it takes to heat water is calculated following the equation below. The rated power of the HP is noted by P_{HP}.

$$T_{\mathrm{heat}} = \frac{0.35 \cdot E_{\mathrm{d}}}{0.4 \cdot P_{\mathrm{HP}} \cdot COP} \tag{5.2}$$

This calculated time is used to control the power consumption, which can be explained in the following way:

1. $t = 0$: The storage starts heating the water, and the power is ramped up to its nominal value.

2. $t = 30min$: The power consumption has reached nominal value.

3. $t = T_{\mathrm{heat}}$: The power consumption is ramped down.

4. $t = T_{\mathrm{heat}} + 30min$: The storage stops consuming power.

To give a better understanding of the control explained above, it has been illustrated on Figure 5.3, which shows how the power consumption as a function of time.
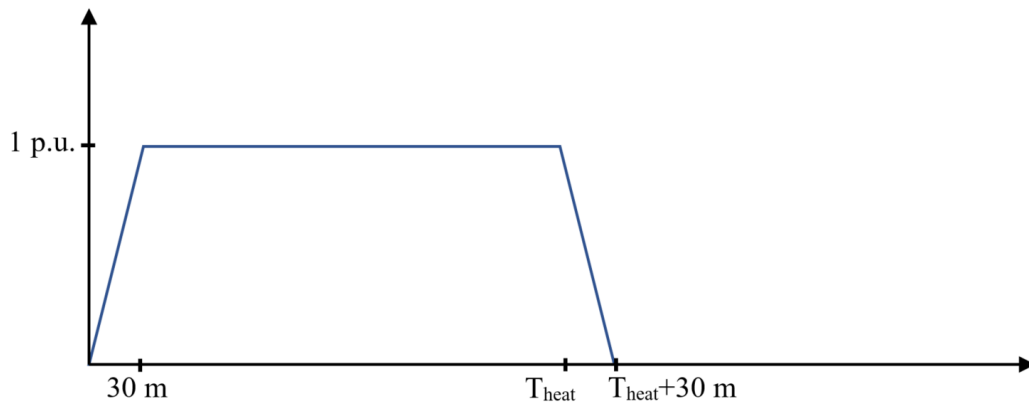
Figure 5.3: The charging strategy of the HWST.

5.2.3 Base load

The aggregated HP system is assumed to always have a base load that corresponds to 65 % of the total energy demand. This is modelled like shown in the lowest block of Figure 5.3. The base power can be calculated using Equation 5.3, where E_{d} is the total energy demand and COP is the coefficient of performance.

$$P_{\text{base}} = \frac{E_{\text{d}} \cdot 0.65}{24 \cdot COP} \tag{5.3}$$

Actual fluctuations of the thermal demand have been ignored in the designed model.

5.2.4 Validation of HP model

The HP model has been validated for a winter day, by using a random a test signal for the LFC. The used test signal can be seen on Figure 5.4 together with the ON/OFF signal.
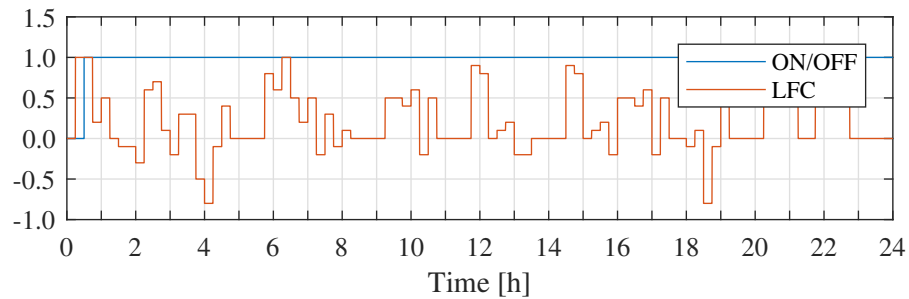
Figure 5.4: Test and ON/OFF signal for HP model validation.

Figure 5.5 shows the original power consumption, and the power consumption with LFC regulation. The original consumption behaves like expected. There is a base load and the storage operation is visible. This original power consumption, with varying T_{heat} has been added to the load profiles for all the simulations. The test signal contains a value above 0 before the 30 minutes have passed, but it can been seen that this signal is ignored and it does not start to regulate before the limit set. When the LFC signal is positive the consumption is decreased and when it is negative it is increased. Additionally, it is clear that there is always a base consumption. The HP model has hereby been validated.
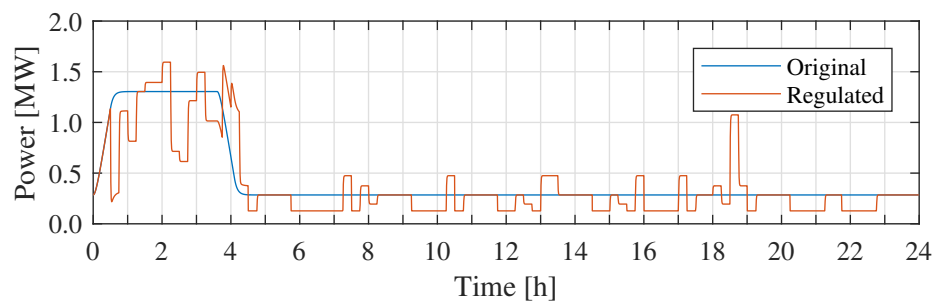
Figure 5.5: Validation of HP model.

5.3 Simulation Results

To see how the aggregated HP system contributes to frequency regulations, RMS simulations have been conducted. The results with the HP contributing are compared to when the heat pump is passive, i.e. the results in chapter 4. The results with comparison will be presented in this section. The tested scenarios are the same as in chapter 4 excluding the current scenario, since no HPs are assumed to be installed at this point. The results are presented using figures and tables.

5.3.1 With 5.4 MW WF: Winter

The first simulations presented are with the 5.4 WF implemented during the winter. The HP is set to have a participation factor of 30 % in the LFC control. These 30 % are taken from the CPP, which means that the HPP has the same participation factor in these simulations as it did in the simulations in chapter 4. The frequency is shown in Figure 5.6. In general it can be said that the results without and with frequency regulation from the HP are very similar, but there are some improvements of the frequency response. One of the places where the improvement is visible is at hour 9. In the original response the frequency jumps from 49.84 Hz to 50.38 Hz, and with contribution from the HP the variation is from 50 Hz to 50.18.
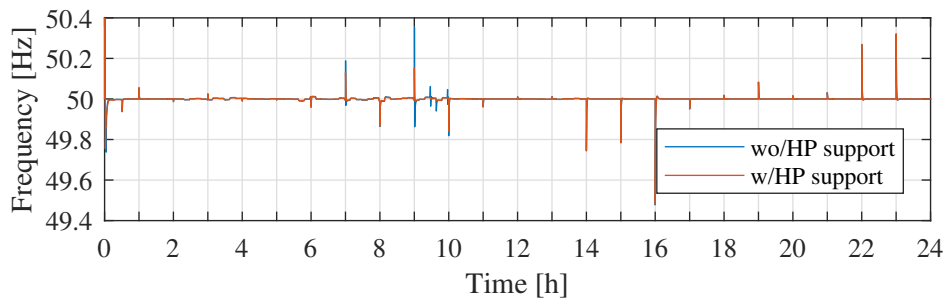
Figure 5.6: The frequency reponse with and without heat pump contribution - winter day with one WF.

Figure 5.7 shows the power of the CPP and the HPP. For the first hours the production varies and this is caused by the wind production. As discussed in chapter 4 the WF is off during the last hours, which cause production from the HPP and CPP to be hourly constant.
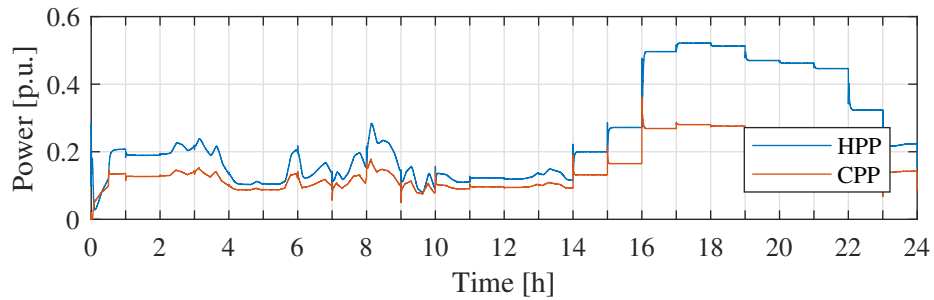
Figure 5.7: The power output of HPP and CPP with heat pump contribution - winter day with one WF.

In Figure 5.8 shows the original HP load and when it is supporting to frequency regulation. The HP contribtuites to regulation over the whole day, even though it is limited by the mininum HP consumption from hour 16 to hour 22.

Figure 5.8: The HP load - winter day with one WF.

5.3.2   With 5.4 MW WF: Summer

For the summer scenario the LFC HP participation factor is set to 25 %. Figure 5.15 shows the frequency response with and without support from the HP. The frequency is actually worse in the first hour with contribution from the HP than without. This can be due the fact that the HP does not start to contribute before 30 minutes have passed. The moment when the when it starts to contribute the frequency drops quite significantly, but this can be due to the sudden increase of load, which is seen on Figure 5.11.

The only time where an improvement of the frequency is noticeable, is at around 1.5 h. Figure 5.11 also shows that the frequency regulation contribution from the HP is minimal. It contributes during the first hours, which is when the wind power production is dominant, as it was showed in Figure 4.10.
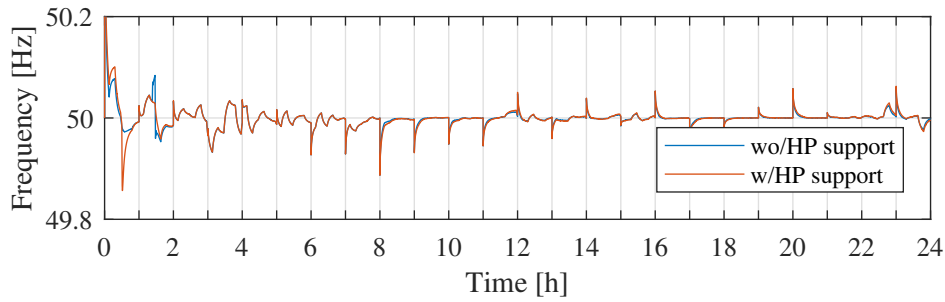
Figure 5.9: The frequency response with and without heat pump contribution - summer day with one WF.

Figure 5.16 shows the CPP and HPP power. The regulation capacity is between 0 and 0.3 pu.
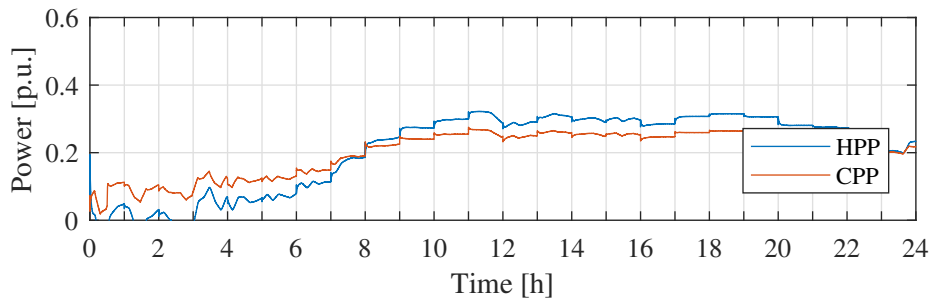
Figure 5.10: The power output of HPP and CPP with heat pump contribution - summer day with one WF.
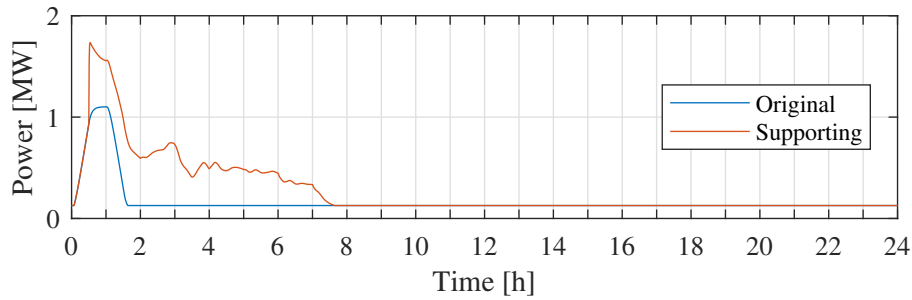
Figure 5.11: The HP load - summer day with one WF.

5.3.3   With 10.8 MW WF: Winter

The next results presented are with a 10.8 MW WF during the winter. The HP's LFC participation was set to 45 %. Again it can be seen that the frequency response is improved,

but not significantly. There are some improvements at hour 6, 11 and 12. The power output of the HPP and CPP can be seen on Figure 5.13.
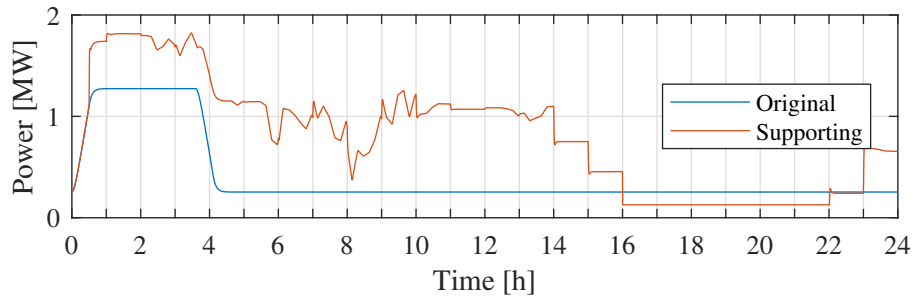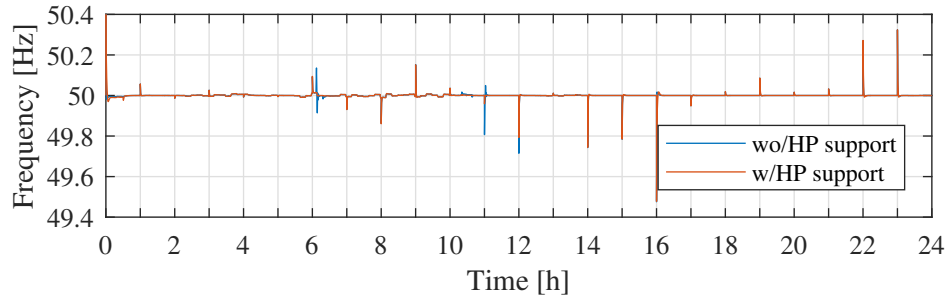

Figure 5.12: The frequency reponse with and without heat pump contribution - winter day with two WFs.
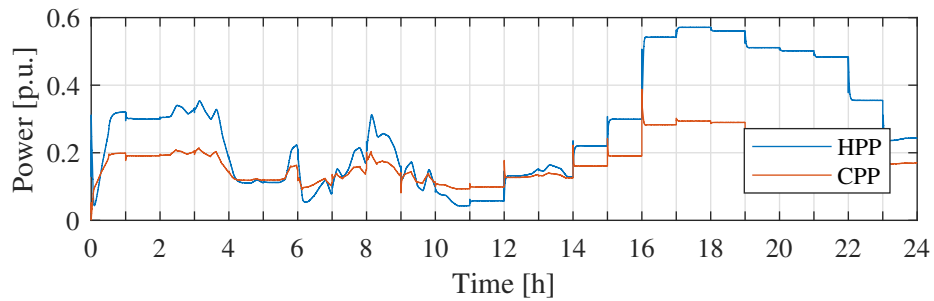
Figure 5.13: The power output of HPP and CPP with heat pump contribution - winter day with two WFs.

The HP power is shown in Figure 5.14. The HP contributes to frequency regulation throughout the day, but similarly to the winter scenario with one WF, it reaches its minimum power consumption at hour 16, and the LFC signal is at this point not capable of regulating the HP power further down.
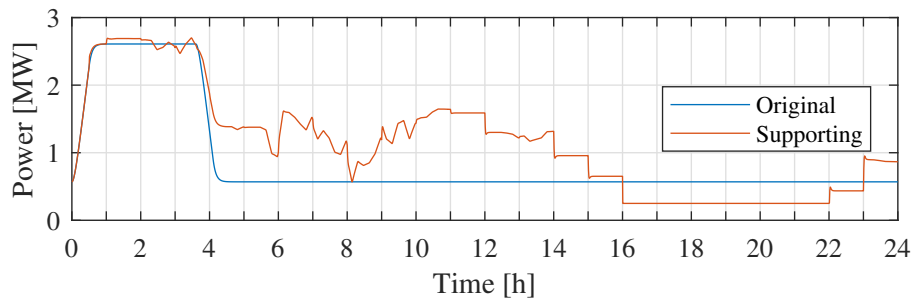
Figure 5.14: The HP load - winter day with two WFs.

5.3.4 With 10.8 MW WF: Summer

The final scenario tested is the summer with a 10.8 MW WF. The frequency is shown on Figure 5.15. This is the only scenario where there are no obvious improvements of the frequency response. Previously it was shown that the frequency was somewhat improved at hour 1.5 for the summer scenario with 1 WF, but in that scenario the frequency was flucating more than it is in this scenario. This is due to the fact that the wind power during the first hour has been increased, and the load has been increased. Thereby, the CPP and HPP contribute with more power during the first hours in this scenario, see Figure 5.16 and Figure 5.10.
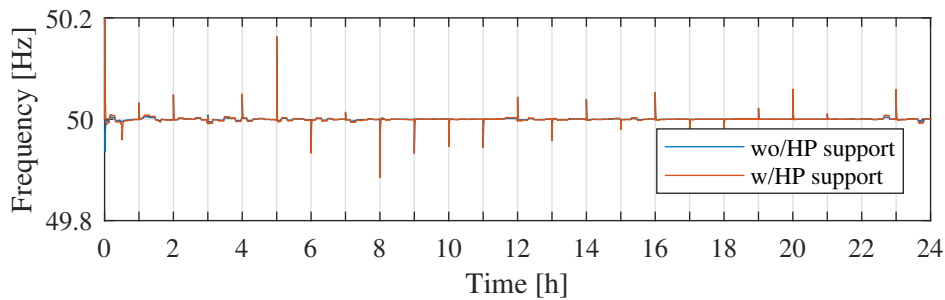
Figure 5.15: The frequency reponse with and without heat pump contribution - summer day with two WFs.
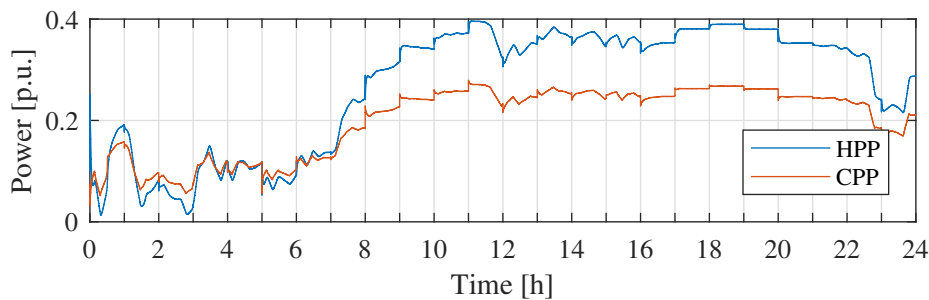
Figure 5.16: The power output of HPP and CPP with heat pump contribution - summer day with two WFs.

Figure 5.17 shows the HP power, and here it is also seen that the power while supporting with frequency regulation is similar to the original HP power, but with a higher load from hours 0.5 to 7.
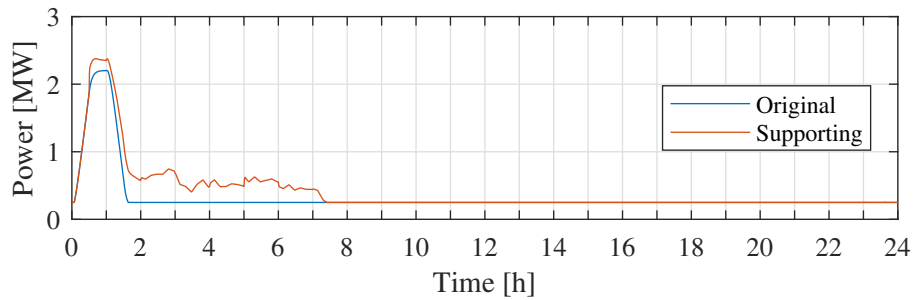
Figure 5.17: The HP load - summer day with two WFs.

In addition to the shown results, tests were made to see if it was possible to increase the amount of WTs online when the HP was contributing to regulation compared to when the HP was passive, but this was not possible. If this would have been possible a higher utilization of the wind turbines would have been achieved due to the LFC control of the HP.

In Table 5.4 the minimum and maximum frequencies for simulations with and without frequency regulation contribution from the HPs are tabulated. By just looking at the minimum and maximum frequencies, it looks like the improvements on the frequency are negligible for all tested scenarios, as the best improvement is a decrease of 0.03 Hz. Even though the maximum and minimum frequencies have not been improved, the figures shown earlier did show some improvements where the frequency was either decreased or increased as desired.

| Scenario | Season | $f_{\min}$ | | $f_{\max}$ | |
		wo/HP	w/HP	wo/HP	w/HP
1 WF	Winter	49.48	49.47	50.35	50.32
	Summer	49.89	49.85	50.27	50.27
2 WF	Winter	49.48	49.48	50.32	50.32
	Summer	49.88	49.89	50.16	50.16

Table 5.4: Simulations results summarized.

The LFC participation factors for the tested scenarios are summarized in Table 5.5.

Scenario	Season	HPP	CPP	HP
1 WF	Winter	0.23	0.42	0.35
	Summer	0.23	0.52	0.25
2 WFs	Winter	0.28	0.32	0.40
	Summer	0.28	0.47	0.25

Table 5.5: LFC participation factors.

5.4 Conclusion

This chapter has introduced a HP model with a LFC signal, that has been implemented in a grid to see how the HP can contribute with frequency regulation. The model was validated, but when it was integrated into the grid, it only improved the frequency response slightly, and not in a significant manner. It is likely that this is due to the limitations of the designed model. The model is restricted with a $\pm40\%$ regulation capacity, the total consumption can never go below 5 % of the rated capacity and it is equipped with a dead band. All of these factors have an impact on how much the heat pump can contribute. The frequency does not fluctuate a lot, as the wind shares are 50 % and below, and the load is hourly based. If a load profile with a higher resolution was obtained the frequency would likely vary more, and therefore there would be a higher need for the regulation of the HP, so this could also make an impact on the improvement of the frequency response. Previous studies have shown that this model has actually been able to improve the frequency response more, than this investigation has shown. Therefore there is a possibility that the model can not be directly applied a grid that is this small compared to the system it was designed for. It was also tested if the wind power utilization could be improved when the HP is contributing to the frequency regulation, but this could not be done.

Chapter 6

Conclusions

This thesis has investigated the contribution HP can bring to frequency regulation. The study has been based on the island power system of Suðuroy, The Faroe Islands.

First, the power grid and the heating sector of the Faroe Islands were introduced. This was followed by some basic frequency regulation theory and a state of the art review regarding this topic. This showed that with the vision of a highly renewable future, it will be necessary to consider flexible loads for frequency regulation, and that this is a topic of high interest.

The test grid has been modelled with a hydro generator, diesel generator, loads and a wind turbine. A load frequency controller has been modelled, and it was shown by simulations that it was capable of restoring the frequency back 50 Hz after the occurrence of a power deficit.

The frequency response of the system has been tested with different amounts of wind power integrated to the system using dynamic simulations. The simulations were conducted based on a winter day and a summer day. First the grid was tested only with a given load profile and the hydro and diesel units. Later wind power was integrated in two stages: 5.4 MW and 10.8 MW. For the simulations during the winter without wind power the frequency fluctuated between 49.87 Hz and 50.07 Hz, and when a wind farm was introduced to the system this range expanded to <49.5 Hz to 50.3 Hz. This shows that wind power has a great impact on the frequency of a power system.

It has also been shown that installing two wind farms of 5.4 MW will bring the potential production from the wind farm well above the actual demand. This means that the wind turbines will have to be curtailed, in order to obtain a balanced power system. The daily wind share varied between 18 % and 50 %.

A heat pump model with a controller was also investigated, modelled, and a understanding of the basic behavior of a heat pumps was achieved. The model developed was aggregated in a realistic and easy way. The model's behavior was validated, but when this heat pump model was integrated into the grid for frequency control it barely improved

the frequency. This is likely due to the restrictions of the designed controller. Additionally, the frequency variations were relatively small, and therefore there was not much room for improvement of them.

The overall conclusion is that HP can contribute to frequency regulation; however, with this specific study case, the developed models and with the data given for the investigation, the improvement was almost negligible.

6.1   Future Works

There several aspects relevant to this project that could be investigated further. First of all; the study case could be investigated using a load profile with a higher resolution, to achieve a more varying frequency, and therefore a better chance to improve it. Simulations could also be conducted for other scenarios than the ones tested in this thesis, e.g. for days with average wind speeds, instead of the two days tested here, where one day had especially high wind speed while the other had very low wind speeds.

It would also be interesting to research which modifications to the grid would be necessary, to be able to increase the wind power shares above 50 %, e.g. by increasing the inertia of the system by implementing a synchronous generator, a battery system etc., so that the system would not be as fragile as it currently is.

A HP model designed specifically for small power systems, could possibly results in a higher contribution of frequency regulation. This is another aspect that could be studied.

In addition to everything mentioned above, it would also be interesting to investigate how other flexible loads like e.g. electric vehicles could contribute to secondary frequency regulation.

References

[1] IRENA, "Renewable energy statistics 2017," Abu Dhabi, United Arab Emirates, 2017.

[2] H. Djuurhus, "Grøna kósin," Feb. 2015, accessed: 2018-03-02. [Online]. Available: http://www.sev.fo/Files//Filer/Um_sev/fradgreidingar/Gronakosin.pdf

[3] The Government of the Faroe Islands, "Coalition agreement," Tórshavn, the Faroe Islands, Sep. 2015.

[4] T. Nielsen, "Technical and economic assessment of a 100 % renewable electricity sector in the faroe islands in 2030, from the power company perspective," Master's thesis, Beuth University of Applied Sciences Berlin, Germany, May 2016.

[5] The Power Company SEV, "Vindur og sól eru vegurin fram," http://www.sev.fo/Default.aspx?ID=8&Action=1&NewsId=2960&PID=6, Apr. 2018, accessed: 2018-04-23.

[6] Agency for the Cooperation of Energy Regulators, "Framework guidelines on electricity grid connections," Ljubljana, Slovenia, Jul. 2011.

[7] V. Kumar, A. S. Pandey, and S. K. Sinha, "Grid integration and power quality issues of wind and solar energy system: A review," in *2016 International Conference on Emerging Trends in Electrical Electronics Sustainable Energy Systems (ICETEESES)*, March 2016, pp. 71–80.

[8] D. M. Pérez and A. R. Dalmau, "Application of power to gas (p2g) systems in danish electric distribution networks," Master's thesis, Aalborg University, Denmark, May 2015.

[9] HyUnder, "Assessment of the potential, the actors and relevant business case for large scale and long term storage of renewable electricity by hydrogen underground storage in europe." last accessed: 2018-03-09. [Online]. Available: http://www.hyunder.eu/

[10] J. M. J. S. J. Lund, Peter D.; Lindgren, "Review of energy system flexibility measures to enable high levels of variable renewable electricity," *Renewable and Sustainable Energy Reviews; Volume 45*, pp. 785–807, 2015.

[11] U. Uslu and B. Zhang, "Energy storages and flexible loads to support large wind power penetration," Master's thesis, Aalborg University, Denmark, Jun. 2016.

[12] T. Masuta and A. Yokoyama, "Supplementary load frequency control by use of a number of both electric vehicles and heat pump water heaters," *IEEE Transactions on Smart Grid*, vol. 3, no. 3, pp. 1253–1262, Sep. 2012.

[13] J. Hong, C. Johnstone, J. Torriti, and M. Leach, "Discrete demand side control performance under dynamic building simulation: A heat pump application," *Renewable Energy*, vol. 39, no. 1, pp. 85–95, 2012.

[14] The Electrical Power Company SEV, "The power supply system," http://www.sev.fo/Default.aspx?ID=124, accessed: 2018-02-25.

[15] ——, "Gjaldskrá," http://www.sev.fo/Default.aspx?ID=34, Jan. 2018, accessed: 2018-02-20.

[16] Heilsu- og innlendismálaráðið, "Løgtingsmál nr. 102/2017: Uppskot til løgtingslóg um broyting í løgtingslóg um framleiðslu, flutning og veiting av ravmangi (elveitingarlógin)," Mar. 2018, note: Bill about differentiating the electricity price.

[17] "Hagtalsgrunnurin," http://www.hagstova.fo/fo/hagtalsgrunnur, accessed: 2018-02-16.

[18] Kári Mortensen, Head of the Energy Directory at the Faroese Environmental Agency, Mar. 2018.

[19] I. Diaz de Cerio Mendaza, B. Bak-Jensen, and Z. Chen, "Electric boiler and heat pump thermo-electrical models for demand side management analysis in low voltage grids," *International Journal of Smart Grid and Clean Energy*, vol. 2, no. 1, pp. 52–59, 2013.

[20] GREENMATCH, "Gjaldskrá," https://www.greenmatch.co.uk/blog/2014/07/how-do-air-source-heat-pumps-work, Jul. 2014, accessed: 2018-03-20.

[21] SUNSHINE RENEWABLE ENERGY, "Efficiency of heat pumps vs oil furnaces in nova scotia," https://www.sunshinerenewables.ca/heat-pump-vs-oil-furnace/, Dec. 2018, accessed: 2018-03-05.

[22] F. N. K. Højgaard, D. P. Nielsen, G. Skála, H. G. Mortensen, and T. Magnussen, "Vitjan hjá Fjarhitafelagnum - samandráttur," 2013, note: A summary from a student excursion.

[23] Nordic Energy Research, "Heat Supply in Leirvík," COWI A/S, Kongens Lyngby, Denmark, Tech. Rep. 1, Nov. 2016.

[24] A. Oudalov, D. Chartouni, and C. Ohler, "Optimizing a battery energy storage system for primary frequency control," *IEEE Transactions on Power Systems*, vol. 22, no. 3, pp. 1259–1266, Aug 2007.

[25] H. Saadat, *Power System Analysis*. McGraw-Hill, 2009. [Online]. Available: https://books.google.dk/books?id=NTSAtgAACAAJ

[26] J. Z. A. D. D.-G. D. Apostolopoulou, Y. C. Chen and P. W. Sauer, "Effects of various uncertainty sources on automatic generation control systemsk," department of Electrical and Computer Engineering, University of Illinois at Urbana-Champaign.

[27] ENTSO-e, "Demand response - system frequency control," Oct. 2017.

[28] The Power Company SEV, "Tekniske krav for tilslutning af produktionsanlæg større end 11 kW til det Færøske elnet," May 2017.

[29] Y. J. Kim, L. K. Norford, and J. L. Kirtley, "Modeling and analysis of a variable speed heat pump for frequency regulation through direct load control," *IEEE Transactions on Power Systems*, vol. 30, no. 1, pp. 397–408, Jan 2015.

[30] Y. J. Kim, E. Fuentes, and L. K. Norford, "Experimental study of grid frequency regulation ancillary service of a variable speed heat pump," *IEEE Transactions on Power Systems*, vol. 31, no. 4, pp. 3090–3099, July 2016.

[31] I. D. de Cerio Mendaza, "An interactive energy system with grid, heating and transportation systems," Ph.D. dissertation, Aalborg University, Aalborg, Denmark, Aug. 2014.

[32] D. Fischer and H. Madani, "On heat pumps in smart grids: A review," *Renewable and Sustainable Energy Reviews*, vol. 70, no. 1364-0321, pp. 342 – 357, 2017.

[33] T. S. Pedersen, P. Andersen, K. M. Nielsen, H. L. Stærmose, and P. D. Pedersen, "Using heat pump energy storages in the power grid," in *2011 IEEE International Conference on Control Applications (CCA)*, Sept 2011, pp. 1106–1111.

[34] DIgSILENT, "PowerFactory 2018 - User Manual," Gomaringen, Germany, Feb. 2018.

[35] Terji Nielsen, Head of the R&D Department at the Power Company SEV, Apr. 2018.

[36] S. Yee, J. Milanović, and F. Hughes, "Phase compensated gas turbine governor for damping oscillatory modes," *Electric Power Systems Research*, vol. 79, no. 8, pp. 1192 – 1199, 2009.

[37] J. Keljik, *Electricity 3 - Power Generation and Delivery*, 9th ed.   DELMAR CENGAGE Learning, 2009.

[38] P. Kundur, N. J. Balu, and M. G. Lauby, *Power system stability and control*.   McGraw-Hill, 2009.

[39] Energinet.dk, "Technical Regulation for Thermal Power Station Units of 1.5 MW and higher," Oct. 2008.

[40] B. Thomsen, "Vindmyllulundin í Suðuroy dregur út," Feb. 2018, last accessed: 17-05-2018. [Online]. Available: https://kvf.fo/netvarp/uv/2018/02/03/vindmylla

[41] G. M. Masters, *Renewable and efficient electric power systems*, 2nd ed.   John Wiley & Sons, Inc., 2013.

[42] Norconsult A/S, "Vindturbiner på Færøyene," Norconsult A/S, Sandvika, Norway, Tech. Rep., 2010.

[43] ENERCON, "The most suitable wind turbine for every location - ENERCON product overview," Aurich, Germany, Jun. 2015, last accessed: 01-05-2018. [Online]. Available: https://www.enercon.de/fileadmin/Redakteur/Medien-Portal/broschueren/pdf/en/ENERCON_Produkt_en_06_2015.pdf

[44] Viessmann, "Vitocal air-to-water heat pump technical guide," 2009, technical Manual.

Appendix A

PowerFactory Models and Data

This appendix contains information about the AVR and governor models used in the simulations. Block diagrams and parameters are represented.

A.1   Automatic Voltage Regulator

The HPP and the CPP are equipped with the same type AVR. The block diagram of the AVR is shown in Figure A.1, and the parameters are tabulated in Table A.1.
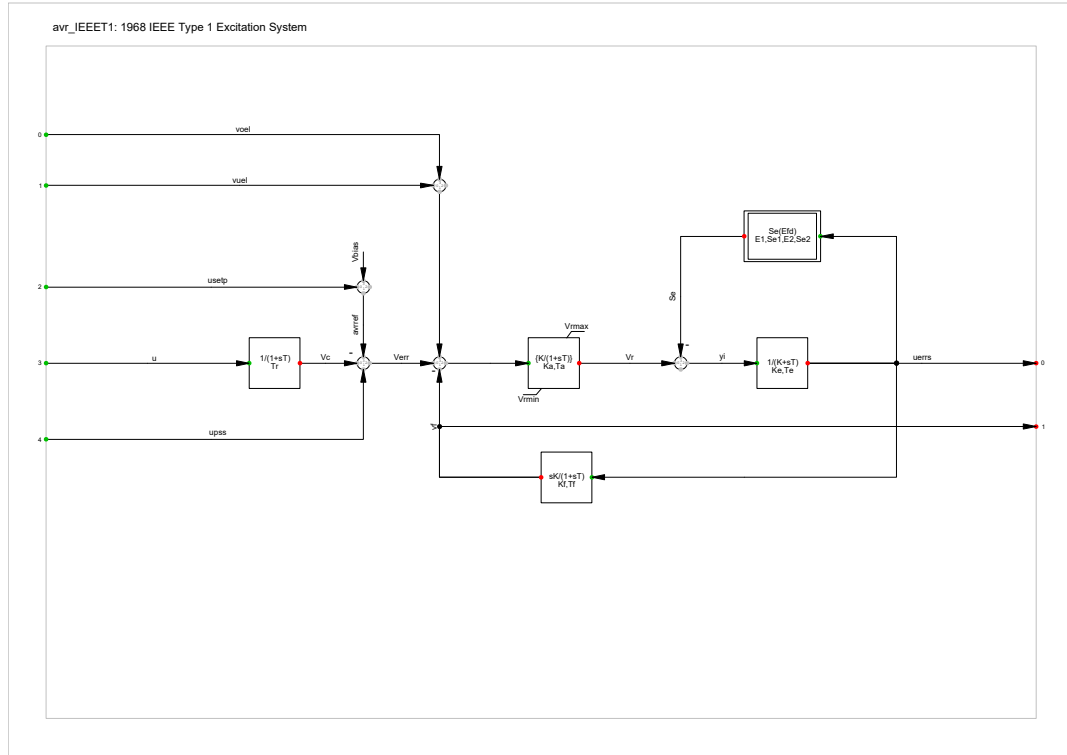
Figure A.1: Block diagram of the used AVR.

Table A.1: The AVR parameters.

Symbol	Description	HPP	CPP
Tr	Measurement Delay [s]	0.02	
Ka	Controller Gain [pu]	200	
Ta	Controller Time Constant [s]	0.03	
Ke	Exciter Constant [pu]	1	
Te	Exciter Time Constant [s]	0.2	
Kf	Stabilization Path Gain [pu]	0.05	
Tf	Stabilization Path Time Constant [s]	1.5	
E1	Saturation Factor 1 [pu]	3.9	
Se1	Saturation Factor 2 [pu]	0.1	
E2	Saturation Factor 3 [pu]	5.2	
Se2	Staturation Factor 4 [pu]	0.5	
Vrmin	Controller Output Minimum [pu]	-10	
Vrmax	Controller Output Maximum [pu]	10	

A.2 Hydro Turbine Governor

The hydro governor is depicted in Figure A.2, and the parameters are shown in Table A.2.

Figure A.2: Block diagram of the hydro governor.

Table A.2: The hydro governor parameters.

Symbol	Description	HPP
R	Permanent Droop [pu]	0.04
r	Temporary Droop [pu]	0.5
Tr	Governor Time Constant [s]	8.408
Tf	Filter Time Constant [s]	0.05
Tg	Servo Time Constant [s]	0.5
Tw	Water Starting Time [s]	0.496
At	Turbine Gain [pu]	1.15
Pturb	Turbine Rated Power(0=pturb=pgen) [MW]	3.12
Dturb	frictional losses factor pu [pu]	0
qnl	No Load Flow [pu]	0.08
Gmin	Minimum Gate Limit [pu]	0
Qnl	No Load Flow [pu]	0
Velm	Gate Velocity Limit [pu]	0.2
Gmax	Maximum Gate Limit [pu]	1

A.3   Thermal Governor

Figure A.3 and Table A.3 represent the thermal governor.

Figure A.3: Block diagram of the thermal governor.

Table A.3: The thermal governor parameters.

Symbol	Description	CPP
R	Droop [pu]	0.047
T1	Controller Time Constant [s]	0.4
T2	Actuator Time Constant [s]	0.1
T3	Compressor Time Constant [s]	3
AT	Ambient Temperature Load Limit [pu]	1
Kt	Turbine Factor [pu]	2
Dturb	Frictional losses factor [pu]	0
Pturb	Turbine Rated Power(0=pturb=pgen) [MW]	0
Vmin	Controller Minimum Output [pu]	0
Vmax	Controller Maximum Output [pu]	1

Appendix B

LFC parameters

The parameters of the LFC are shown in Table B.1, Table B.2, Table B.3 and Table B.4.

K	0.5
T	10

Table B.1: LFC gain and time delay.

Unit	Capacity	LFC Participation	Frequency Bias Factor
CPP	13.28	0.81	5.65
HPP	3.12	0.19	1.56

Table B.2: LFC parameters without wind power.

Unit	Capacity	LFC Participation	Frequency Bias Factor
CPP	10.72	0.77	4.56
HPP	3.12	0.23	1.56

Table B.3: LFC parameters with one wind farm.

Unit	Capacity	LFC Participation	Frequency Bias Factor
CPP	8.16	0.72	3.47
HPP	3.12	0.28	1.56

Table B.4: LFC parameters with two wind farms.

Appendix C

Heat Pump Model

The capacities of the CPP and the HPP and the frequency bias factors are as represented in Appendix B. The LFC participation factors were are tabulated in Table 5.5. Other parameters of the LFC HP control are represented here in the tables below, Table C.1 and Table C.2.

Minimum Total Power	0.1275 MW
Maximum Total Power	2.55 MW
Dead band	± 0.02 MW
Control delay, T_{hpc}	30 s
Start delay, T_{start}	300 s
Regulating capacity limit	± 1.02 MW

Table C.1: With 1 WF.

Minimum Total Power	0.255 MW
Maximum Total Power	5.1 MW
Dead band	± 0.02 MW
Control delay, T_{hpc}	30 s
Start delay, T_{start}	300 s
Regulating capacity limit	± 2.04 MW

Table C.2: With 2 WFs.